

Anharmonic processes of scattering and absorption of slow quasi-transverse modes in cubic crystals with positive and negative anisotropies of second-order elastic moduli

This article has been downloaded from IOPscience. Please scroll down to see the full text article.

2008 J. Phys.: Condens. Matter 20 465201

(<http://iopscience.iop.org/0953-8984/20/46/465201>)

View [the table of contents for this issue](#), or go to the [journal homepage](#) for more

Download details:

IP Address: 129.252.86.83

The article was downloaded on 29/05/2010 at 16:35

Please note that [terms and conditions apply](#).

Anharmonic processes of scattering and absorption of slow quasi-transverse modes in cubic crystals with positive and negative anisotropies of second-order elastic moduli

I G Kuleyev, I I Kuleyev and I Yu Arapova

Institute of Metal Physics, Ural Division, Russian Academy of Sciences,
620219 Ekaterinburg, Russia

E-mail: kuleev@imp.uran.ru (I G Kuleyev)

Received 6 May 2008, in final form 18 September 2008

Published 21 October 2008

Online at stacks.iop.org/JPhysCM/20/465201

Abstract

The quasi-transverse ultrasound absorption during anharmonic processes of the scattering in cubic crystals with positive (Ge, Si, diamond and InSb) and negative (KCl and NaCl) anisotropies of the second-order elastic moduli is studied. Mechanisms underlying the relaxation of the slow quasi-transverse mode by two slow (the SSS mechanism) or two fast (the SFF) modes are discussed in the long-wavelength approximation. Angular dependences of the ultrasound absorption for the SSS, SFF and Landau–Rumer relaxation mechanisms are analyzed in terms of the anisotropic continuum model. The full absorption of the slow quasi-transverse mode is determined. It is shown that the SSS and SFF relaxation mechanisms are due to the cubic anisotropy of the crystals, leading to the interaction between noncollinear phonons. Two most important cases—the wavevectors of phonons are in the cube face plane or the diagonal planes—are considered. In crystals with a considerable anisotropy of the elastic energy (Ge, Si, InSb, KCl and NaCl) the total contribution of the SSS and SFF relaxation mechanisms to the full absorption is either several times or one to two orders of magnitude larger than the contribution from the Landau–Rumer mechanism depending on the direction. Much of the dominance of the former relaxation mechanisms over the Landau–Rumer mechanism is explained by second-order elastic moduli.

(Some figures in this article are in colour only in the electronic version)

1. Introduction

The relaxation of quasi-transverse phonons and the ultrasound absorption in cubic crystals with competition of the defect and anharmonic scattering processes was considered in [1, 2]. Dependences of the transverse ultrasound absorption on the wavevector direction were analyzed in terms of the anisotropic continuum model for the Landau–Rumer mechanism [3] when the merging of a transverse and a longitudinal phonon produces a longitudinal phonon ($T + L \rightarrow L$). In accordance with the views established in the literature [1–7], this relaxation mechanism is the main one for transverse phonons in normal three-phonon scattering processes. It was taken as the main mechanism of the relaxation of transverse thermal phonons

in calculating the lattice heat conductivity [8–11]. In the long-wavelength approximation $\hbar\omega_q^\lambda \ll k_B T$ (T being the temperature and $\omega_{q\lambda}$ the frequency of a phonon with a wavevector q and a polarization λ) the Landau–Rumer mechanism gives a well known linear dependence [1–7] of the ultrasound absorption on the wavevector of the form $\alpha_{\text{TLL}}^\lambda \sim qT^4$. Much less attention was attached to the study of anharmonic relaxation processes involving three transverse phonons in different vibrational branches (TTT mechanisms). According to the estimates made in terms of the isotropic medium model [3–7], these relaxation processes are inefficient. Firstly, transverse modes are degenerate in the case of isotropic media and only collinear phonons can participate in TTT mechanisms [1–4]. If the dispersion

of phonons is taken into account, the probability of the phonon scattering for this scattering mechanism becomes zero. Therefore, relaxation processes involving three transverse phonons can take place in isotropic media only if the damping of phonon states is taken into account, with the damping effect dominating over the dispersion effect [4–7]. Secondly, it was shown [12] that in isotropic media the matrix element of the interaction between collinear phonons and, correspondingly, the ultrasound absorption in TTT mechanisms become zero. However, the isotropic medium approximation [3–11], which is commonly used to estimate the probability of various scattering processes, is inadequate for germanium, silicon, diamond and other semiconductor crystals having cubic symmetry and a considerable anisotropy both of the harmonic and the anharmonic energy. It should be noted that the anisotropy of the spectrum and the presence of degeneracy points in vibrational modes of transverse phonons lead to considerably different rates of the relaxation of longitudinal phonons in some anharmonic processes of scattering in cubic crystals as compared to isotropic media [13, 14]. A convenient approximation for the study of anharmonic relaxation processes is the anisotropic continuum model. In this model, the harmonic energy of cubic crystals is expressed as three second-order elastic moduli, while the anharmonic energy as six third-order elastic moduli. The second- and third-order elastic moduli have been determined experimentally for a number of cubic crystals. Therefore, the phonon relaxation rates calculated in terms of this model present a reliable basis for the interpretation of experimental data on the ultrasound absorption and the phonon transport in cubic crystals.

The ultrasound absorption during anharmonic relaxation processes involving three transverse phonons was studied in [15–17]. However, the approximations used in [15–17] are inadequate for cubic crystals. Firstly, the researchers disregard the intersections between the spectra of quasi-transverse vibrational branches, leading to an abrupt (stepwise) change of the group velocity in the vicinity of those intersections. Secondly, the effect of the cubic anisotropy on the phonon polarization is not considered in the matrix element of the three-phonon scattering processes: the vibrational modes are assumed to be purely transverse modes as in isotropic media. The procedure of averaging over directions of polarization vectors in the matrix element, which they use in this case, is incorrect for cubic crystals. Thirdly, the ultrasound absorption is calculated for all symmetric directions, but the form of the conservation law adopted by the researchers allows the correct analysis of the [001] direction only (see appendix). Because of this restriction, the full picture is obscure and optimal directions, in which the transverse ultrasound absorption is maximum and minimum, cannot be determined.

It is known [4, 18] that quasi-longitudinal or quasi-transverse vibrations propagate in cubic crystals, while pure modes propagate only in symmetric directions such as [100], [110] and [111]. The analysis of the spectrum and the polarization of vibrational branches [19] demonstrated that the contribution of the transverse component to quasi-longitudinal vibrations in cubic crystals is small and can be neglected. Conversely, the contribution of the longitudinal components to

Table 1. Thermodynamic elasticity moduli for the cubic crystals under study, in 10^{12} dyne cm^{-2} . The data are adopted from [4, 27].

	Ge	Si	Diamond	InSb	KCl	NaCl
c_{11}	1.289	1.657	10.76	0.672	0.398	0.487
c_{12}	0.483	0.638	1.25	0.367	0.062	0.124
c_{44}	0.671	0.796	5.758	0.302	0.0625	0.126
ΔC	0.54	0.57	2.01	0.3	-0.211	-0.11
$k - 1$	0.87	0.67	0.4	0.81	-0.63	-0.31
c_{111}	-7.10	-8.25	-62.6	-3.56	-7.01	-8.8
c_{112}	-3.89	-4.51	-22.6	-2.66	-0.571	-0.571
c_{123}	-0.18	-0.64	1.12	-1.0	0.284	0.284
c_{144}	-0.23	0.12	-6.74	0.16	0.127	0.257
c_{155}	-2.92	-3.10	-28.6	-1.39	-0.245	-0.611
c_{456}	-0.53	-0.64	-8.23	-0.004	0.118	0.271
\tilde{c}_{155}	-1.63	-1.9	-5.4	-1.54	-0.61	-1.41
\tilde{c}_{111}	28.01	32.4	138.1	20.96	1.62	8.23
\tilde{c}_{112}	-3.25	-4.1	-10.24	-1.98	-1.11	-1.37
$c_{456} + c_{44}$	0.14	0.156	-2.47	0.31	0.181	0.397
$\tilde{c}_{155} - \Delta C$	-2.17	-2.47	-7.41	-1.84	-0.4	-1.3

the quasi-transverse modes is not small and the longitudinal component of these modes should be considered in the relaxation rates of quasi-transverse phonons when averaging over the polarization vectors. Thus, the approximations used in [15–17] can lead to large errors in calculating the relaxation rate of transverse phonons. In the present study the effect of the cubic anisotropy on the spectrum and the polarization of phonons are taken into account exactly. It was shown [19] that the anisotropy of the elastic energy in cubic crystals is determined by the dimensionless parameter $k - 1 = \Delta C / (c_{11} - c_{44})$ (here $\Delta C = c_{12} + 2c_{44} - c_{11}$, with c_{ij} being second-order elastic moduli). The parameters $k - 1$ and ΔC have like signs. Then all cubic crystals can be classified into those with the positive ($\Delta C > 0$) and the negative ($\Delta C < 0$) anisotropy of the second-order elastic moduli. This parameter is zero in isotropic media. The first type includes Ge, Si, diamond, InSb, GaSb, GaAs, and other crystals. KCl, NaCl, CaF_2 , etc crystals are referred to the second type [19] (see table 1). The detailed analysis of elastic waves in cubic crystals [19] demonstrated that the physical basis of the classification proposed in [19] is the qualitatively different anisotropy of the spectra and the behavior of polarization vectors in cubic crystals of the two types. The formal anisotropy factor $A = 2c_{44} / (c_{11} - c_{12})$, which was introduced in [20], also characterizes the elastic anisotropy of cubic crystals. However, it does not appear in either the equation for the spectra of vibrational branches or the definition of the polarization vectors (see below). It should be noted that the sign of the parameter $A - 1 = \Delta C / (c_{11} - c_{12})$ coincides with the sign of ΔC . It was shown [17, 18] that in cubic crystals of the first and second types not only the spectrum and polarization vectors of phonons, but also the behavior of relaxation characteristics, such as the ultrasound absorption and the relaxation rate of quasi-transverse vibrational modes, are qualitatively different for both the scattering by defects and the Landau–Rumer mechanism.

In what follows we shall consider processes of the merging of an ultrasound wave and a transverse thermal phonon, leading to the formation of a transverse thermal phonon like

$T_1^{\lambda} + T_2^{\lambda_1} \rightarrow T_3^{\lambda_1}$ (TTT mechanisms) (λ and λ_1 being the phonon polarizations that acquire two values, t_1 as the fast quasi-transverse mode and t_2 as the slow quasi-transverse mode). These scattering processes can lead to dependences of the absorption of long-wavelength transverse phonons of the slow mode having the same form as the Landau–Rumer mechanism, $\alpha_{\text{TTT}}^{t_2} \approx qT^4$, and, hence, can compete with this mechanism [3]. We shall show further that the TTT relaxation mechanisms involve both collinear and noncollinear phonons, with the greatest contribution made by the scattering to large angles. Since such scattering processes are impossible in isotropic media, it can be stated that anharmonic relaxation processes involving three transverse phonons in such crystals as Ge, Si, diamond, InSb, etc are due exclusively to the cubic anisotropy of these crystals. So, the quasi-transverse ultrasound absorption by the TTT mechanism should be calculated taking into account the anisotropy of both the harmonic and the anharmonic energy of the crystals.

We shall analyze angular dependences of the quasi-transverse ultrasound absorption by TTT mechanisms for two types of cubic crystals with positive (Ge, Si, diamond and InSb) and negative (KCl and NaCl) anisotropies of second-order elastic moduli. Values of the TTT absorption will be compared with those for the Landau–Rumer mechanism [2]; the full absorption for the slow quasi-transverse mode will be determined. Unlike [15–17], we shall analyze angular dependences of the ultrasound absorption for two most important cases, namely (1) the sound wavevectors in the cube face plane, and (2) those in the diagonal plane, making it possible to determine optimal directions, in which the absorption of the slow quasi-transverse mode reaches the maximum and minimum. Considering the results obtained in [12] for isotropic media, we shall discuss in detail the problem of the scattering of collinear and noncollinear phonons in cubic crystals and their role in the ultrasound absorption.

2. Absorption of quasi-transverse ultrasound in cubic crystals during anharmonic scattering processes

If the inequality $\omega_{q\lambda}\tau^\lambda(\mathbf{q}, T) \gg 1$ ($\tau^\lambda(\mathbf{q}, T) = 1/\nu^\lambda(\mathbf{q}, T)$ and $\omega_{q\lambda}$ being the frequency of a phonon with a wavevector \mathbf{q} and a polarization λ) is fulfilled, the ultrasonic wave absorption $\alpha_\lambda(\mathbf{q})$ with a wavevector \mathbf{q} and a polarization λ is proportional to the full relaxation rate of phonons of the given polarization $\nu^\lambda(\mathbf{q}, T)$ (see, e.g., [2, 4]):

$$\alpha_\lambda(\mathbf{q}, T) = \frac{4.34\nu^\lambda(\mathbf{q}, T)}{S_\lambda(\mathbf{q})}(\text{dB cm}^{-1}), \quad (1)$$

where $S_\lambda(\mathbf{q}) = S_\lambda(\theta, \varphi)$ is the phonon phase velocity, which depends on the angular variables θ and φ of the vector \mathbf{q} , and T is the temperature. Experimental studies of the ultrasound absorption [4, 21] demonstrated that the inequality $\omega_{q\lambda}\tau^\lambda(\mathbf{q}, T) \gg 1$ is fulfilled at sufficiently low temperatures: below 50, 100 and 300 K for germanium, silicon and diamond crystals respectively. Here we shall restrict ourselves to the absorption of the long-wavelength transverse ultrasound when $\hbar\omega_{qt} \ll k_B T$. In what follows we shall only consider the intervals of temperatures and wavevectors \mathbf{q} over which these

inequalities hold. If the inequality $\omega_{q\lambda}\tau^\lambda(\mathbf{q}, T) \gg 1$ is fulfilled, the dominant contribution to the volume absorption of ultrasonic waves is due to the scattering by defects, including the isotopic scattering and normal processes of the phonon–phonon scattering (see, e.g., [4]). The scattering by defects is considered in [2]. Here we shall restrict ourselves to the analysis of anharmonic relaxation processes involving three quasi-transverse phonons.

The possible variants of the relaxation of transverse phonons in cubic crystals are the following processes of the merging of two transverse phonons, which is followed by the formation of a transverse phonon:

$$\begin{aligned} (1) \quad & \text{ST}_1 + \text{ST}_2 \rightarrow \text{ST}_3 & \text{FT}_1 + \text{FT}_2 \rightarrow \text{FT}_3, \\ & \omega_{q_1}^\lambda = \omega_{q_3}^\lambda - \omega_{q_2}^\lambda, \\ (2) \quad & \text{ST}_1 + \text{FT}_2 \rightarrow \text{FT}_3, & \omega_{q_1}^{t_2} = \omega_{q_3}^{t_1} - \omega_{q_2}^{t_1}, \\ & \text{FT}_1 + \text{ST}_2 \rightarrow \text{ST}_3, & \omega_{q_1}^{t_1} = \omega_{q_3}^{t_2} - \omega_{q_2}^{t_2} \quad (2) \\ (3) \quad & \text{FT}_1 + \text{FT}_2 \rightarrow \text{ST}_3, & \omega_{q_1}^{t_1} = \omega_{q_3}^{t_2} - \omega_{q_2}^{t_1}, \\ (4) \quad & \text{FT}_1 + \text{ST}_2 \rightarrow \text{FT}_3, & \omega_{q_1}^{t_1} = \omega_{q_3}^{t_1} - \omega_{q_2}^{t_2}, \\ & \text{ST}_1 + \text{ST}_2 \rightarrow \text{FT}_3, & \omega_{q_1}^{t_2} = \omega_{q_3}^{t_1} - \omega_{q_2}^{t_2}. \end{aligned}$$

The processes (1) involve three transverse phonons belonging to either the upper (FT, $\lambda = t_1$) or the lower (ST, $\lambda = t_2$) vibrational branch. It was already noted that collinear phonons can only participate in the processes (1) in isotropic media [4–7]. If the dispersion of phonons is taken into account, the probability that phonons are scattered through this scattering mechanism tends to zero. It should be noted that the dispersion of the transverse vibrational branches is very appreciable in such crystals as Ge, Si and InSb. Processes like (1) can take place in isotropic media if the damping of phonon states is considered. In this case, the damping should dominate over the dispersion [4–7]. The correct analysis of the effect of the damping of phonon states in the TTT mechanisms requires finding the total relaxation frequency of transverse thermal phonons, which is determined by all relaxation processes. The analysis of this mechanism [7] for isotropic media taking into account the damping of phonon states gives the wavevector-independent absorption $\alpha_{\text{TTT}}^\lambda \sim q^0 T^4 \nu(T)$. We shall show that in the case of the processes (1) $\text{ST}_1 + \text{ST}_2 \rightarrow \text{ST}_3$ (the SSS mechanism) the energy conservation law is strictly fulfilled for noncollinear phonons too. They give dependences of the long-wavelength ultrasound absorption of the same form as those for the Landau–Rumer mechanism: $\alpha_{\text{SSS}}^\lambda \sim qT^4$. It will be shown that in many cubic crystals this mechanism makes the predominant contribution to the full absorption of the slow quasi-transverse mode. The processes like (2) (the SFF mechanism) are analogous to processes of the relaxation of transverse phonons in the case of the Landau–Rumer mechanism. They give dependences of the long-wavelength ultrasound absorption of the form $\alpha_{\text{SFF}}^{t_2} \sim qT^4$ and can also compete with the Landau–Rumer mechanism [2, 4]. In the processes (2) the energy of a scattered transverse phonon equals the difference of the energies of phonons belonging to one and the same transverse vibrational branch. Obviously,

this mechanism is impossible in isotropic media because the transverse branches are degenerate and the phonon spectrum is isotropic. Therefore, the higher is the cubic anisotropy (the more the parameter k differs from unity), the more efficient are the relaxation mechanisms connected with processes like (1) and (2). The type (3) processes are impossible because the energy conservation law cannot be fulfilled for these processes. Processes like (4) are analogous to processes of the relaxation of longitudinal phonons through the Herring mechanism [13, 14] ($L_1 + ST_2 \rightarrow FT_3$, $\omega_{q_1}^L = \omega_{q_3}^{t_1} - \omega_{q_2}^{t_2}$). In the processes (4) the energy of a scattered transverse phonon equals the difference of the energies of the upper and lower transverse vibrational branches. This mechanism leads to the dependence of the long-wavelength transverse ultrasound absorption of the form $\alpha_{TTT}^\lambda \sim q^2 T^3$, which is less efficient in the long-wavelength approximation than the one for the Landau–Rumer mechanism, $\alpha_{TLL}^\lambda \sim q T^4$ [3]. In what follows we shall present calculations of the absorption of slow quasi-transverse modes for the processes (1) and (2) in cubic crystals. Then it will be possible to determine the full absorption of slow quasi-transverse modes as the long-wavelength approximation. Other variants of the relaxation of ST modes leading to the dependence of the Landau–Rumer type are unavailable.

The initial expression for the relaxation rate of phonons with a polarization λ_1 has the form [9]

$$\nu_{\text{phN}}(q_1, \lambda_1) = \frac{\pi \hbar^4}{(2\rho k_B T)^3} \frac{1}{V} \sum_{\substack{\mathbf{q}_2 \mathbf{q}_3 \\ \lambda_2 \lambda_3}} \frac{sh\left(\frac{z_1}{2}\right) \cdot \delta_{\mathbf{q}_1 + \mathbf{q}_2 + \mathbf{q}_3, 0}}{z_1 z_2 z_3 sh\left(\frac{z_2}{2}\right) sh\left(\frac{z_3}{2}\right)} \\ \times \left| V_{\mathbf{q}_1 \mathbf{q}_2 \mathbf{q}_3}^{\lambda_1 \lambda_2 \lambda_3} \right|^2 \left\{ 2\delta(\omega_{q_1 \lambda_1} + \omega_{q_2 \lambda_2} - \omega_{q_3 \lambda_3}) \right. \\ \left. + \delta(\omega_{q_1 \lambda_1} - \omega_{q_2 \lambda_2} - \omega_{q_3 \lambda_3}) \right\}. \quad (3)$$

Here ρ is the density, V is the normalization volume, T is the temperature, the polarization λ takes two values t_1 and t_2 , and $z_n = \hbar \omega_{q_n}^n / k_B T$. In expression (3) we shall only consider the first term in the braces, in which the merging of two transverse phonons produces a transverse phonon. Processes of the decomposition of a transverse phonon to two transverse phonons are not discussed since they can be considerable for thermal and high-frequency phonons.

In the anisotropic continuum model the spectrum of phonons with a polarization λ and a wavevector much smaller than the Debye wavevector q_d can be written as

$$\omega_q^\lambda = S_\lambda(\theta, \varphi) q. \quad (4)$$

The spectrum anisotropy is determined by the anisotropy of the phase velocity $S_\lambda(\theta, \varphi)$, which depends on the angles θ and φ of the vector \mathbf{q} . In the system of coordinates connected with the cube edges we have [19]

$$S_\lambda(\theta, \varphi) = \sqrt{\frac{c_{44}}{\rho}} \left(1 + \frac{c_{11} - c_{44}}{c_{44}} \left(\frac{1}{3} + Z_\lambda \right) \right)^{1/2}, \\ Z_{t_1, t_2} = \frac{2}{3} r \cos\left(\frac{Q}{3} \mp \frac{2\pi}{3}\right), \quad Q = \arccos q, \\ q = \left\{ \frac{1 + 4.5(k^2 - 1)\xi + 13.5\eta(k - 1)^2(2k + 1)}{r^3} \right\}, \\ r = \sqrt{1 + 3(k^2 - 1)\xi}, \quad k = \frac{c_{12} + c_{44}}{c_{11} - c_{44}} \quad (5)$$

where c_{ij} denotes the second-order elastic moduli; $\xi = n_1^2 n_2^2 + n_1^2 n_3^2 + n_2^2 n_3^2$ and $\eta = n_1^2 n_2^2 n_3^2$ are cubic harmonics; $\mathbf{n} = \mathbf{q}/q = (\sin(\theta) \cos(\varphi), \sin(\theta) \sin(\varphi), \cos(\theta))$ is a unit wavevector of a phonon. The indices t_1 and t_2 correspond to the ‘fast’ (the upper) and the ‘slow’ (the lower) transverse vibrational modes. The polarization vectors of phonons in different vibrational branches are defined by the expressions [14]

$$e_j^\lambda = \frac{1}{A_\lambda} \left\{ \frac{n_j}{\psi_j^\lambda} \right\}, \quad A_\lambda = \pm \sqrt{\sum_j \frac{n_j^2}{(\psi_j^\lambda)^2}}, \quad (6) \\ (\mathbf{e}^\lambda \mathbf{n}) = \frac{1}{A_\lambda} \sum_j \frac{n_j^2}{\psi_j^\lambda}, \quad \psi_j^\lambda = \varepsilon_\lambda + (k - 1)n_j^2.$$

It is seen from (5) and (6) that just the parameter $k - 1$ characterizes the influence of the elastic anisotropy on the spectrum and polarization vectors of vibrational modes in cubic crystals. The analysis [19] revealed that the contribution of longitudinal components to the quasi-transverse modes is not small. According to [19], the maximum contribution is 16.5% in Ge, 10% in Si, 8% in diamond, and up to 27% in KCl crystals. Therefore, in what follows we shall calculate the absorption considering the contribution of the longitudinal component to transverse–longitudinal vibrations as an approximation linear in this component. To determine the velocity $S_\lambda(\theta_3, \varphi_3)$ from the momentum conservation law, we shall express the angular variables θ_3 and φ_3 of the vector \mathbf{q}_3 as the angular variables θ_1, φ_1 and θ_2, φ_2 of the wavevectors \mathbf{q}_1 and \mathbf{q}_2 , and find the corresponding cubic harmonics:

$$\xi_3 = (1 - \psi_3)\psi_3 + \psi_4^2, \quad \eta_3 = \psi_3 \psi_4^2, \\ \psi_3 = (\cos \theta_3)^2 \\ = (\cos \theta_2 + y \cos \theta_1)^2 / (1 + y^2 + 2y \cos \theta_{12}), \\ y = q_1 / q_2, \quad (7) \\ \psi_4 = (\sin \theta_3)^2 \sin \varphi_3 \cos \varphi_3 \\ = \frac{(\sin \theta_2 \sin \varphi_2 + y \sin \theta_1 \sin \varphi_1)}{(1 + y^2 + 2y \cos \theta_{12})} \\ \times (\sin \theta_2 \cos \varphi_2 + y \sin \theta_1 \cos \varphi_1), \\ \cos \theta_{12} = (\mathbf{n}_1 \mathbf{n}_2) = \sin \theta_1 \cos(\varphi_2 - \varphi_1) \sin \theta_2 + \cos \theta_1 \cos \theta_2. \quad (8)$$

In the long-wavelength limit $\hbar \omega_{q_i} \ll k_B T$ ($q_1 \ll q_2, q_3$) at temperatures much lower than the Debye temperature the integral over z_2 in (3) is calculated exactly, and for the ultrasound absorption in the SSS ($\lambda_1 = t_2$ and $\lambda_2 = \lambda_3 = t_2$) and SFF ($\lambda_1 = t_2$ and $\lambda_2 = \lambda_3 = t_1$) processes we have

$$\alpha_{TTT}^{t_2}(\theta_1, \varphi_1, T) = A_{TTT}^{t_2} z_1^{t_2} T^5, \\ A_{TTT}^{t_2} = A_{SSS}^{t_2} + A_{SFF}^{t_2} = A_{0TTT}^{t_2} J_{TTT}^{t_2}(\theta_1, \varphi_1) \text{ (dB cm}^{-1} \text{ K}^{-5}\text{)}, \\ J_{TTT}^{t_2}(\theta_1, \varphi_1) = J_{SSS}^{t_2}(\theta_1, \varphi_1) + J_{SFF}^{t_2}(\theta_1, \varphi_1), \quad (9) \\ A_{SSS}^{t_2}(\theta_1, \varphi_1) = A_{0TTT}^{t_2} J_{SSS}^{t_2}(\theta_1, \varphi_1), \\ A_{SFF}^{t_2}(\theta_1, \varphi_1) = A_{0TTT}^{t_2} J_{SFF}^{t_2}(\theta_1, \varphi_1), \quad z_1^2 = \frac{\hbar \omega_{q_1}^{\lambda_1}}{k_B T},$$

$$A_{0\text{TTT}}^{t2} = \frac{4.34\pi^3 k_B^5}{15\hbar^4 \rho^3 (S_{t2}(\theta_1, \varphi_1))^2 (S_{100}^t)^8}, \quad (10)$$

$$S_{100}^t = \left(\frac{c_{44}}{\rho}\right)^{1/2}$$

$$J_{\text{TTT}}^{\lambda_1}(\theta_1, \varphi_1) = \sum_{\lambda_2} \int_{-1}^1 dx \frac{1}{\pi} \int_0^{2\pi} d\varphi_2 \delta(\cos\theta_{12} - S_{\lambda_1\lambda_2\lambda_2}^{**})$$

$$\times \frac{I_{\text{TTT}}^{\lambda_1\lambda_2\lambda_2}(\theta_1, \varphi_1, \theta_2, \varphi_2)}{(\tilde{S}_2^{\lambda_2})^8}, \quad x = \cos\theta_2 \quad (11)$$

$$S_{\lambda_1\lambda_2\lambda_2}^{**} = \frac{\tilde{S}_1^{\lambda_1}}{\tilde{S}_2^{\lambda_2}} - \Delta_{\lambda_2},$$

$$\Delta_{\lambda_2}(\theta_1, \varphi_1, \theta_2, \varphi_2) = \lim_{y \rightarrow 0} \left\{ \frac{1}{y} \left[\frac{\tilde{S}_3^{\lambda_2} - \tilde{S}_2^{\lambda_2}}{\tilde{S}_2^{\lambda_2}} \right] \right\}. \quad (12)$$

$$\tilde{S}_1^{\lambda_1} = \frac{S_1^{\lambda_1}}{S_{100}^t}, \quad y = \frac{q_1}{q_2}.$$

The exact expression for the matrix element of the three-phonon scattering processes [2, 22] will only include the terms that are linear in longitudinal components of quasi-transverse vibrations, while the terms proportional to quadratic combinations of $(\mathbf{e}_1\mathbf{n}_1)$, $(\mathbf{e}_2\mathbf{n}_2)$, $(\mathbf{e}_3\mathbf{n}_3)$ will be neglected. The error of this approximation is about 1% in Ge, InSb, GaSb and GaAs, and less than 1% in Si and diamond. Then for the square of the matrix element in the long-wavelength approximation ($q_2 \cong q_3$ and $n_2 \cong n_3$) we have for all the relaxation variants (1)–(4)

$$I_{\text{TTT}}^{\lambda_1\lambda_2\lambda_3}(\theta_1, \varphi_1, \theta_2, \varphi_2) = \frac{1}{4} \left\{ \tilde{c}_{111} \sum_i e_{1i} e_{2i} e_{3i} n_{1i} n_{2i}^2 \right.$$

$$+ \tilde{c}_{112} \sum_i [e_{1i} e_{2i} n_{1i} n_{2i} (\mathbf{e}_3\mathbf{n}_3)$$

$$+ e_{1i} e_{3i} n_{1i} n_{2i} (\mathbf{e}_2\mathbf{n}_2) + e_{2i} e_{3i} n_{2i}^2 (\mathbf{e}_1\mathbf{n}_1)]$$

$$+ \tilde{c}_{155} \sum_i [e_{1i} e_{2i} e_{3i} (n_{1i} + 2 \cos\theta_{12} n_{2i})$$

$$+ e_{1i} e_{2i} n_{2i} [n_{1i} (\mathbf{e}_3\mathbf{n}_2) + n_{2i} (\mathbf{e}_3\mathbf{n}_1)]$$

$$+ e_{1i} e_{3i} n_{2i} [n_{1i} (\mathbf{e}_2\mathbf{n}_2) + n_{2i} (\mathbf{e}_2\mathbf{n}_1)]$$

$$+ e_{2i} e_{3i} n_{1i} 2n_{2i} (\mathbf{e}_1\mathbf{n}_2)]$$

$$+ (\tilde{c}_{155} - \Delta c) \sum_i n_{1i} n_{2i}^2 [e_{1i} (\mathbf{e}_2\mathbf{e}_3)$$

$$+ e_{2i} (\mathbf{e}_1\mathbf{e}_3) + e_{3i} (\mathbf{e}_1\mathbf{e}_2)]$$

$$+ (c_{144} + c_{456}) [(\mathbf{e}_2\mathbf{n}_2)(\mathbf{e}_3\mathbf{n}_1)(\mathbf{e}_1\mathbf{n}_3) + (\mathbf{e}_3\mathbf{n}_3)(\mathbf{e}_1\mathbf{n}_2)(\mathbf{e}_2\mathbf{n}_1)]$$

$$+ (c_{12} + c_{144}) [(\mathbf{e}_2\mathbf{e}_3)(\mathbf{e}_1\mathbf{n}_1) + (\mathbf{e}_1\mathbf{e}_3)(\mathbf{e}_2\mathbf{n}_2) \cos\theta_{12}$$

$$+ (\mathbf{e}_1\mathbf{e}_2)(\mathbf{e}_3\mathbf{n}_3) \cos\theta_{12}]$$

$$+ (c_{44} + c_{456}) [(\mathbf{e}_2\mathbf{e}_3)(\mathbf{e}_1\mathbf{n}_2) 2 \cos\theta_{12} + (\mathbf{e}_1\mathbf{e}_2)[(\mathbf{e}_3\mathbf{n}_1)$$

$$+ (\mathbf{e}_3\mathbf{n}_2) \cos\theta_{12}] + (\mathbf{e}_1\mathbf{e}_3)((\mathbf{e}_2\mathbf{n}_1) + (\mathbf{e}_2\mathbf{n}_2) \cos\theta_{12}) \left. \right\}^2, \quad (13)$$

where

$$\tilde{c}_{112} = c_{112} - c_{123} - 2c_{144}, \quad \tilde{c}_{155} = c_{155} - c_{144} - 2c_{456},$$

$$\tilde{c}_{111} = c_{111} - 3c_{112} + 2c_{123} + 12c_{144} - 12c_{155} + 16c_{456},$$

$$\Delta C = c_{12} + 2c_{44} - c_{11}, \quad (14)$$

where c_{ijk} denotes thermodynamic third-order elastic moduli and $\mathbf{e}_{1,2,3}$ stands for polarization vectors. Notice that the terms including third-order elastic moduli \tilde{c}_{111} , \tilde{c}_{112} , \tilde{c}_{155} and ΔC correspond to the anisotropic scattering. These terms distinguish cubic crystals from an isotropic medium: they turn to zero when changing to the isotropic medium model. The other terms in the formula (13) correspond to the isotropic scattering. The expression for the matrix element (13) allows analysis of the absorption of quasi-transverse modes with all the relaxation variants in TTT mechanisms. In the specific case of the relaxation processes (1) and (2) the expression (13) for the square of the matrix element is considerably simplified because in the long-wavelength approximation at $\mathbf{n}_2 \cong \mathbf{n}_3$ and $\lambda_2 = \lambda_3$ we have $\mathbf{e}_2 \cong \mathbf{e}_3$. Then

$$I_{\text{TTT}}^{\lambda_1\lambda_2\lambda_2}(\theta_1, \varphi_1, \theta_2, \varphi_2) = \frac{1}{4} \left\{ \tilde{c}_{111} \sum_i e_{1i} e_{2i}^2 n_{1i} n_{2i}^2 \right.$$

$$+ \tilde{c}_{112} \sum_i [2e_{1i} e_{2i} n_{1i} n_{2i} (e_2 n_2) + e_{2i}^2 n_{2i}^2 (\mathbf{e}_1\mathbf{n}_1)]$$

$$+ \tilde{c}_{155} \sum_i [e_{1i} e_{2i}^2 (n_{1i} + 2n_{2i} \cos\theta_{12})$$

$$+ 2e_{1i} e_{2i} n_{2i} [n_{1i} (\mathbf{e}_2\mathbf{n}_2) + n_{2i} (\mathbf{e}_2\mathbf{n}_1)] + 2e_{2i}^2 n_{1i} n_{2i} (\mathbf{e}_1\mathbf{n}_2)]$$

$$+ (\tilde{c}_{155} - \Delta c) \sum_i [n_{1i} n_{2i}^2 (e_{1i} + 2e_{2i} (\mathbf{e}_1\mathbf{e}_2))]$$

$$+ 2(c_{144} + c_{456}) (\mathbf{e}_2\mathbf{n}_2) (\mathbf{e}_2\mathbf{n}_1) (\mathbf{e}_1\mathbf{n}_2)$$

$$+ (c_{12} + c_{144}) [(\mathbf{e}_1\mathbf{n}_1) + 2(\mathbf{e}_1\mathbf{e}_2) (\mathbf{e}_2\mathbf{n}_2) \cos\theta_{12}]$$

$$+ 2(c_{44} + c_{456}) [(\mathbf{e}_1\mathbf{n}_2) \cos\theta_{12} + (\mathbf{e}_1\mathbf{e}_2)$$

$$\times [(\mathbf{e}_2\mathbf{n}_1) + (\mathbf{e}_2\mathbf{n}_2) \cos\theta_{12}] \left. \right\}^2. \quad (15)$$

In the approximation of pure modes $(\mathbf{e}_2\mathbf{n}_2) = (\mathbf{e}_1\mathbf{n}_1) = 0$, which is discussed in [12], we obtain

$$I_{\text{TTT}}^{\lambda_1\lambda_2\lambda_2}(\theta_1, \varphi_1, \theta_2, \varphi_2) = \frac{1}{4} \left\{ \tilde{c}_{111} \sum_i e_{1i} e_{2i}^2 n_{1i} n_{2i}^2 \right.$$

$$+ \tilde{c}_{155} \sum_i [e_{1i} e_{2i}^2 (n_{1i} + 2n_{2i} \cos\theta_{12})$$

$$+ 2e_{1i} e_{2i} n_{2i}^2 (\mathbf{e}_2\mathbf{n}_1) + 2e_{2i}^2 n_{1i} n_{2i} (\mathbf{e}_1\mathbf{n}_2)]$$

$$+ (\tilde{c}_{155} - \Delta c) \sum_i n_{1i} n_{2i}^2 [e_{1i} + 2e_{2i} (\mathbf{e}_1\mathbf{e}_2)]$$

$$+ 2(c_{44} + c_{456}) [(\mathbf{e}_1\mathbf{n}_2) \cos\theta_{12} + (\mathbf{e}_1\mathbf{e}_2) (\mathbf{e}_2\mathbf{n}_1)] \left. \right\}^2. \quad (16)$$

Notice that in an arbitrary direction of the wavevector q_1 the matrix element (16) includes a term proportional to the third-order elastic modulus \tilde{c}_{111} . This modulus is one order of magnitude larger than the other third-order moduli in the majority of cubic crystals, but its sign is opposite to the sign of the initial modulus c_{111} (see [22], table 1). It is responsible for the small deviation of the relaxation characteristics in cubic crystals from those calculated in the context of the isotropic medium model [12]. When changing to the isotropic medium model, which is discussed in [12], the terms including the third-order elastic moduli \tilde{c}_{111} , \tilde{c}_{155} and ΔC become zero and, hence, only the last term remains in (16), which determines the matrix element for the isotropic medium. The result obtained in [12] becomes obvious from this expression. For the

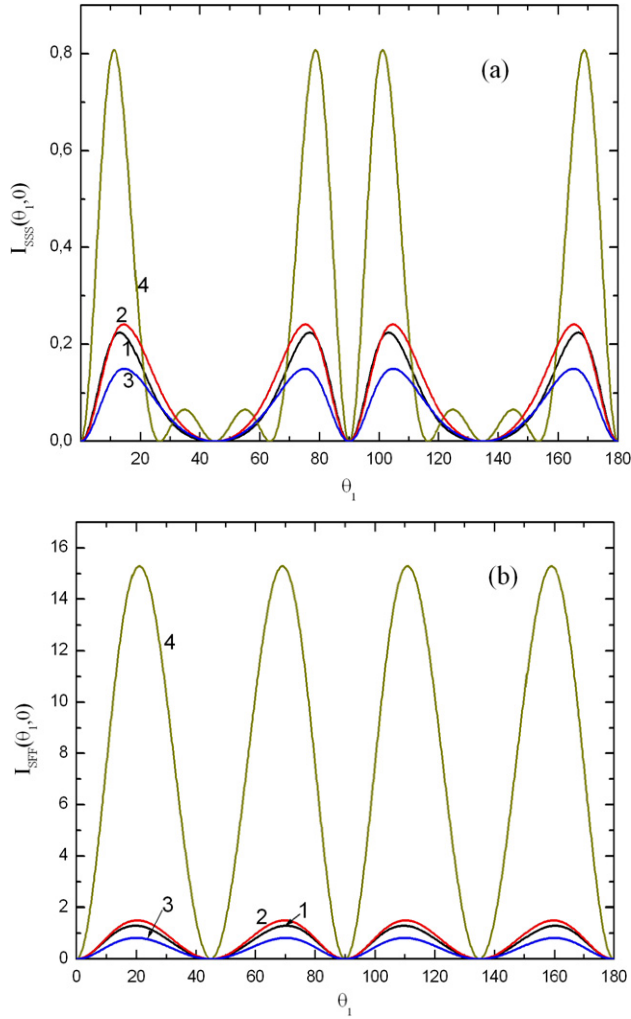


Figure 1. Angular dependences of the square of the matrix element during the scattering of collinear phonons in the SSS (a) and SFF (b) relaxation mechanisms for sound wavevectors in the cube face plane in Ge (1), Si (2), InSb (3) and diamond (4).

scattering of collinear phonons $\mathbf{n}_1 = \mathbf{n}_2$ and the matrix element identically turns to zero because isotropic media pass pure modes when $(\mathbf{e}_2 \mathbf{n}_2) = (\mathbf{e}_1 \mathbf{n}_1) = 0$. Thus, for the scattering of collinear phonons in isotropic media the square of the matrix element identically turns to zero in an arbitrary direction of the wavevector of a phonon.

The situation is considerably different for the cubic crystals. The consideration of the cubic anisotropy of the harmonic and anharmonic energies of the crystals leads to nonzero values of the matrix element (15) for the scattering of collinear phonons via the SSS and SFF relaxation mechanisms only when the slow ST mode is a quasi-transverse mode whose longitudinal component is nonzero. The square of the matrix element is zero if the slow ST mode is a purely transverse mode. As can be seen from figures 1(a) and (b), in the case of the wavevectors lying in the cube face plane and the scattering of collinear phonons the squares of the matrix elements for the SSS ($I_{\text{TTT}}^{t_2 t_2 t_2}(\theta_1, 0, \theta_1, 0) \equiv I_{\text{SSS}}(\theta_1, 0)$) and SFF ($I_{\text{TTT}}^{t_1 t_1 t_1}(\theta_1, 0, \theta_1, 0) = I_{\text{SFF}}(\theta_1, 0)$) relaxation mechanisms are nonzero. They turn to zero in the [001] and [101] directions in all the crystals of the first group.

An exception is the diamond crystal, for which the function $I_{\text{SSS}}(\theta_1, 0)$ becomes zero additionally at the angles $\theta_1 = \pi/4 \pm \pi/10$. These zeros are due to the mutual compensation of the terms proportional to different elastic moduli in (15) and an anomalously large value of the third-order elastic modulus \tilde{c}_{111} in diamond (see table 1). Conversely, in all the crystals of the second group (including KCl and NaCl) the square of the matrix element for the SSS and SFF relaxation mechanisms is zero at all values of the angle θ_1 . This is because in the crystals of the second group the slow ST mode for the wavevectors in the cube face plane is a purely transverse mode with the polarization vector being perpendicular to the cube face under consideration (see [19]). It is easy to check that for this mode $e_{1i} n_{1i} = 0$ at all i and, therefore, expression (15) becomes zero for the scattering of collinear phonons ($\mathbf{n}_1 = \mathbf{n}_2$). In the case of the wavevectors lying in the diagonal plane ($\varphi_1 = \pi/4$), the square of the matrix element $I_{\text{TTT}}^{t_2 t_2 t_2}(\theta_1, \pi/4, \theta_1, \pi/4) = I_{\text{SSS}}(\theta_1, \pi/4)$ is nonzero in the crystals of the first group (Ge, Si, diamond and InSb) at the angles $0 < \theta_1 < \theta_{111}$ and $\pi - \theta_{111} < \theta_1 < \pi$ (θ_{111} being the angle between the z -axis and the [111] direction) (see figure 2(a)). In this case, the slow ST mode is a quasi-transverse mode with the polarization vector in the diagonal plane. At the angles $\theta_{111} < \theta_1 < \pi - \theta_{111}$ the slow ST mode is a pure mode with the polarization vector being perpendicular to the diagonal plane and the function $I_{\text{SSS}}(\theta_1, \pi/4)$ turns to zero (see figure 2(a)). In the crystals of the second group the square of the matrix element $I_{\text{SSS}}(\theta_1, \pi/4)$ is nonzero at the angles $\theta_{111} < \theta_1 < \pi - \theta_{111}$ (the mode t_2 is a quasi-transverse mode with the polarization vector lying in the diagonal plane) and is zero at $0 < \theta_1 < \theta_{111}$ and $\pi - \theta_{111} < \theta_1 < \pi$ (the mode t_2 is a pure mode with the polarization vector being perpendicular to the diagonal plane) (see [19]). The same situation occurs for the SFF relaxation mechanism (see figure 2(b)). With the wavevectors in the diagonal plane ($\varphi_1 = \pi/4$), the square of the matrix element $I_{\text{TTT}}^{t_1 t_1 t_1}(\theta_1, \pi/4, \theta_1, \pi/4) = I_{\text{SFF}}(\theta_1, \pi/4)$ for the SFF relaxation mechanism is nonzero at the angles $0 < \theta_1 < \theta_{111}$ and $\pi - \theta_{111} < \theta_1 < \pi$ in the crystals of the first group and at the angles $\theta_{111} < \theta_1 < \pi - \theta_{111}$ in the crystals of the second group. The above analysis suggests that the angular dependences of the square of the matrix element are qualitatively different for the scattering of collinear phonons in cubic crystals with positive and negative anisotropies of the elastic energy.

Let us compare expression (16) with the result obtained in [16]. For the particular case studied in [16] (the wavevector q_1 is directed along the z -axis ($\mathbf{n}_1 = \{0, 0, 1\}$)), $e_{1i} n_{1i} = 0$ at all i and $\cos \theta_{12} = \cos \theta_2$. The first term in formula (16), which is proportional to the modulus \tilde{c}_{111} , vanishes and we have for the square of the matrix element

$$\begin{aligned}
 I_{\text{TTT}}^{\lambda_1 \lambda_2 \lambda_2}(\theta_1, \varphi_1, \theta_2, \varphi_2) = & \left\{ \tilde{c}_{155} \sum_i [e_{1i} e_{2i}^2 n_{2i} \cos \theta_2 \right. \\
 & + e_{1i} e_{2i} n_{2i}^2 (\mathbf{e}_2 \mathbf{n}_1) + e_{2i}^2 n_{1i} n_{2i} (\mathbf{e}_1 \mathbf{n}_2) \\
 & + (\tilde{c}_{155} - \Delta c) \sum_i n_{1i} n_{2i}^2 e_{2i} (\mathbf{e}_1 \mathbf{e}_2) \\
 & \left. + (c_{44} + c_{456}) [(\mathbf{e}_1 \mathbf{n}_2) \cos \theta_2 + (\mathbf{e}_1 \mathbf{e}_2)(\mathbf{e}_2 \mathbf{n}_1)] \right\}^2. \quad (16a)
 \end{aligned}$$

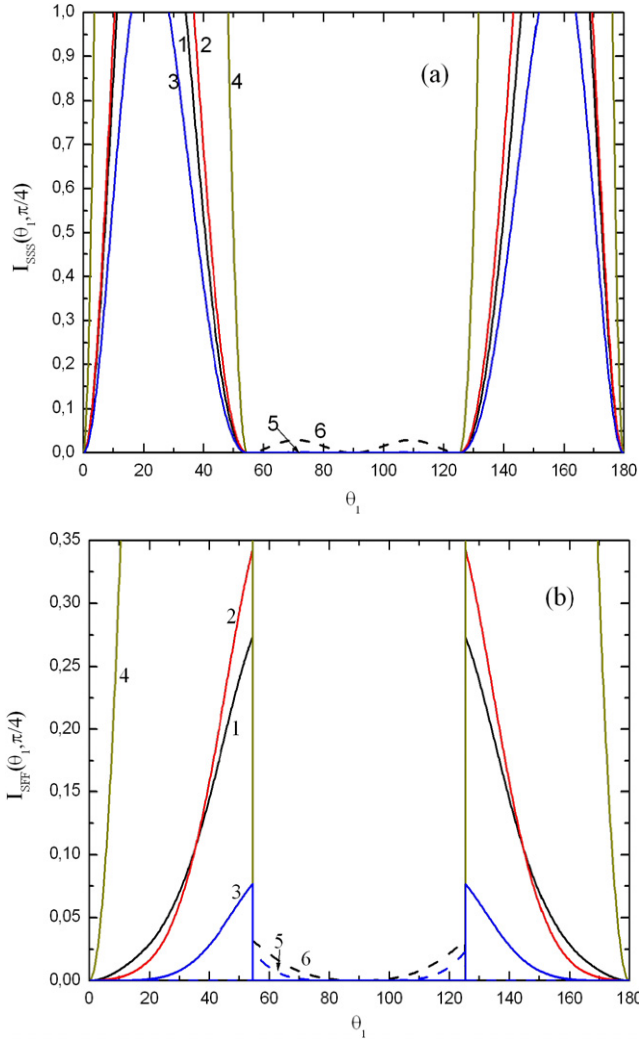


Figure 2. Angular dependences of the square of the matrix element during the scattering of collinear phonons in the SSS (a) and SFF (b) relaxation mechanisms for sound wavevectors in the diagonal plane in Ge (1), Si (2), InSb (3) and diamond (4).

In the notation [16] values $\tilde{c}_{155} = P_1$, $\Delta C = 2D$ and $c_{44} + c_{456} = I$; therefore, in the case of the TTT mechanism expression (16a) includes the same third-order elastic moduli as in [16]. However, the angular dependences of the matrix element (16a) for the TTT mechanism are very different from those in [16]. To verify this, let us determine polarization vectors of the pure modes corresponding to the modes t_1 and t_2 in cubic crystals by the following method [19]:

$$\begin{aligned} \mathbf{e}_0^1 &= (-\sin \varphi, \cos \varphi, 0), \\ \mathbf{e}_0^2 &= (\cos \theta \cos \varphi, \cos \theta \sin \varphi, -\sin \theta), \end{aligned} \quad (17)$$

where the vector \mathbf{e}_0^1 is perpendicular to the plane $\varphi = \text{const}$ and \mathbf{e}_0^2 lies in the plane $\varphi = \text{const}$ and is perpendicular to the vector $\mathbf{n} = (\sin(\theta) \cos(\varphi), \sin(\theta) \sin(\varphi), \cos(\theta))$. Substituting (17) into (16a) gives for the scattering processes

(1) and (2) in directions like [001] ($\theta_1 = 0, \varphi_1 = 0$)

$$I_{\text{TTT}}^{t_2, t_2, t_2}(\theta_1, \varphi_1, \theta_2, \varphi_2) = (\sin \theta_2 \cos \theta_2)^2 \{ P_1 \cos \varphi_2 ((\cos \theta_2)^2 + \sin \theta_2 \cos \theta_2) (\cos \varphi_2)^2 - (P_1 - 2D) (\cos \theta_2)^2 \sin \varphi_2 \}^2$$

$$I_{\text{TTT}}^{t_2, t_1, t_1}(\theta_1, \varphi_1, \theta_2, \varphi_2) = (\sin \theta_2 \cos \theta_2 \cos \varphi_2)^2 \times \{ P_1 (\sin \varphi_2)^2 + I \}^2 \quad (18)$$

$$I_{\text{TTT}}^{t_1, t_2, t_2}(\theta_1, \varphi_1, \theta_2, \varphi_2) = (\sin \theta_2 (\cos \theta_2)^3 \sin \varphi_2)^2 \times \{ P_1 (\cos \varphi_2)^2 + P_1 - 2D \}^2.$$

Notice that in the case of collinear phonons ($\theta_2 = 0, \varphi_2 = 0$) the matrix elements (16) turn to zero similarly to expression (2) in [16]. This is in agreement with the result [12] obtained in the isotropic medium model. The comparison of (18) and expressions (2) in [16] shows that they are considerably different. Firstly, with all the variants of the transverse phonon relaxation via the processes (1) and (2) the author of [16] obtained the same result for the matrix element after two averaging procedures: over the phonon polarization vectors and then over the angles φ_2 . Obviously, the procedure of the matrix element averaging over the phonon polarization vectors [16] is not correct for cubic crystals. Secondly, the averaging of the square of the matrix element over the angles φ_2 in [16] introduces an uncontrolled approximation (see below expressions (19) and (20)). Notice that in the Landau–Rumer mechanism ($T + L \rightarrow L$) the expression for the matrix element derived in [16] is correct [2].

For calculating the integral $J_{\text{TTT}}^{\lambda_1}(\theta_1, \varphi_1)$ in (12), it is necessary first to find solutions to the equation

$$F_{\lambda_1 \lambda_2}(\theta_1, \varphi_1, x, \varphi_2) = \cos \theta_{12} - \left(\frac{\tilde{S}_1^{\lambda_1}}{\tilde{S}_2^{\lambda_2}} - \Delta_{\lambda_2}(\theta_1, \varphi_1, x, \varphi_2) \right) = 0$$

for $-1 \leq x \leq 1, \quad x = \cos \theta_2$ (19)

and take the integral over x using the δ -function (in this case, the roots of equation (19) x_1 become functions of the angles φ_2, θ_1 , and φ_1). Then the expression for $J(\theta_1, \varphi_1)$ assumes the form

$$J_{\text{TTT}}^{\lambda_1}(\theta_1, \varphi_1) = \sum_{\lambda_2, j} \frac{1}{\pi} \int_0^{2\pi} d\varphi_2 \frac{I_{\text{TTT}}^{\lambda_1 \lambda_2 \lambda_2}(\theta_1, \varphi_1, x_j, \varphi_2)}{(\tilde{S}_2^{\lambda_2})^8 |F_j^1|}, \quad (20)$$

$$F_j^1 = \left. \frac{dF(\theta_1, \varphi_1, x, \varphi_2)}{dx} \right|_{x=x_j(\varphi_2, \theta_1, \varphi_1)}.$$

Obviously, if the cubic anisotropy is taken into account in the energy conservation law, the procedure of deriving the roots of equation (19) can only be solved numerically. In the appendix the functions $F_{\lambda_1 \lambda_2}(\theta_1, \varphi_1, \theta_2, \varphi_2)$ and Δ_{λ_2} for arbitrary directions of the wavevectors of phonons are written in terms of the group velocity of phonons. It is shown that the form of the conservation law adopted in [15–17] allows correct analysis of the [001] direction only. Its use for the other symmetric directions is invalid. It should be noted that Δ_{λ_2} is important for relaxation processes (1) and (2): it ensures the

interaction of noncollinear phonons in the SSS mechanism and considerably extends the interval of the angles at which long-wavelength phonons of the mode t_2 can be scattered by thermal phonons of the upper vibrational mode in the SFF mechanism. According to the estimates, in directions like [001] ($\theta_1 = 0$, $\varphi_1 = 0$) and [101] ($\theta_1 = \pi/4$, $\varphi_1 = 0$) the maximum values of Δ_{λ_2} are as large as 0.6 in InSb crystals and 0.18 in diamond. One might expect therefore that in such elastically anisotropic crystals as Ge and InSb ($k = 1.8$) the TTT mechanisms will be more significant than in diamond ($k = 1.4$). The numerical analysis of equation (19) shows that it also possesses solutions for noncollinear phonons in the case of the slow transverse mode and the SSS ($\lambda_1 = t_2$ and $\lambda_2 = t_2$) and SFF ($\lambda_1 = t_2$ and $\lambda_2 = t_1$) relaxation processes. As can be seen from figure 3(a), in directions like [001] ($\theta_1 = 0$, $\varphi_1 = 0$) two solutions exist for the SSS relaxation processes in Ge, Si and InSb crystals: one solution corresponds to the interaction of collinear phonons ($\theta_{12} = \theta_2 = 0$, figure 3(a), curves 5) and the other to the interaction of noncollinear phonons (figure 3(a), curves 1, 2 and 3). The solution corresponding to the interaction of collinear phonons (figure 3(a), curves 5) only exists for the SFF relaxation processes in these crystals. In diamond and NaCl crystals with a lower anisotropy of the harmonic energy the SSS and SFF relaxation processes in directions like [001] can only involve collinear phonons (figure 3(a), curves 5). In KCl crystals, which are more anisotropic, the energy conservation law permits the interaction of both collinear (figure 3(a), curves 5) and noncollinear (figure 3(a), curves 4, 4' and 4'') phonons. Three solutions exist for each of the two relaxation mechanisms. The analysis performed suggests that the dominant contribution to the SSS and SFF relaxation rates in directions like [101] is due to the interaction of noncollinear phonons. In directions like [001] ($\theta_1 = \pi/4$, $\varphi_1 = 0$) the solutions corresponding to the interaction of collinear phonons exist only for the SSS mechanism and are absent for the SFF relaxation mechanism in the crystals under study. It is seen from figure 3(b) that for the SSS mechanism equation (19) possesses solutions corresponding to the scattering to the angles $48^\circ < \theta_{12} < 65^\circ$ (three solution regions, curves 1) and $35^\circ < \theta_{12} < 37^\circ$ (six solution regions, curves 1a) in Ge crystals. Roots which correspond to the scattering to large angles in Ge crystals are absent in Si, while the two domains of roots for the SSS mechanism are much smaller than those in Ge (see the inset in figure 3(b), curves 3). In the case of the SFF relaxation mechanism, the domains of the roots of equation (19), which correspond to the interaction of noncollinear phonons, are nearly equal in Ge and Si crystals (see figure 3(b), curves 2 and 4).

As is shown in [1, 2], a simpler variant is available for calculating the relaxation rates of phonons and this variant eliminates the procedure of finding the roots of equation (19), $F(x, \varphi_2, \theta_1, \varphi_1) = 0$, but requires calculating a double integral $J_{TTT}^\lambda(\theta_1, \varphi_1)$ instead of a single integral. It consists in replacement of the δ -function in expression (11) by its representation as a limiting process from the Lorentzian or

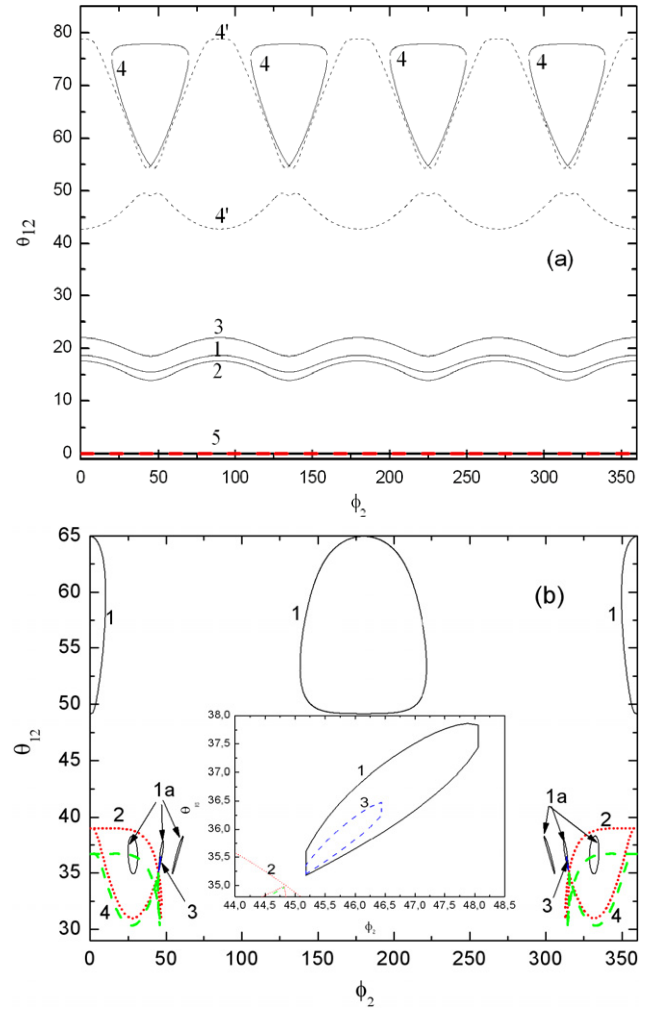


Figure 3. (a) Dependences of the angle θ_{12} between the sound wavevector and a scattered phonon (θ_2 , φ_2) on the angle φ_2 according to equation (19) in crystallographic directions like [001] ($\theta_1 = 0$, $\varphi_1 = 0$): the SSS relaxation mechanism in Ge (1), Si (2), InSb (3), and KCl (4); the SFF relaxation mechanisms in Ge, Si and InSb crystals (curve 5) and in KCl (curves 4', 4'' and 5); the SSS and SFF relaxation mechanisms in diamond and NaCl crystals (curves 5). (b) Dependences of the angle θ_{12} for the sound wavevectors in crystallographic directions like [101] ($\theta_1 = \pi/4$, $\varphi_1 = 0$) on the angle φ_2 according to equation (19): the SSS relaxation mechanisms in Ge (curves 1 and 1a) and Si (3); the SFF relaxation mechanisms in Ge (curves 2) and Si (curves 4).

Gaussian function:

$$\delta(F(x, \varphi_2, \theta_1, \varphi_1)) = \frac{1}{\pi} \lim_{\varepsilon \rightarrow 0} \frac{\varepsilon}{(F(x, \varphi_2, \theta_1, \varphi_1))^2 + \varepsilon^2},$$

$$\delta(F(x, \varphi_2, \theta_1, \varphi_1)) = \lim_{\varepsilon \rightarrow 0} \frac{1}{2\sqrt{\pi\varepsilon}} \times \exp(- (F(x, \varphi_2, \theta_1, \varphi_1))^2 / 4\varepsilon). \quad (21)$$

The numerical analysis demonstrates that both approximations give the same results, but the Gaussian provides a better approximation of the δ -function in calculating the relaxation rates as it considerably curtails the computation time. Notice that the calculated values of $\alpha_{TLL}^\lambda(\theta_1, \varphi_1)$ for the Landau–Rumer mechanism in the variant (21) with the damping are

in agreement with the exact calculations to within the error, which is not over 0.1% at $\varepsilon = 10^{-4}$ [2]. The point is that $S_{\text{TLL}}^{**}(x, \varphi_2, \theta_1, \varphi_1) \leq 1$ for the Landau–Rumer mechanism. The energy conservation law is fulfilled both in the isotropic approximation and with the exact consideration of the cubic anisotropy. With this mechanism, $\Delta_L(\theta_1, \varphi_1, \theta_2, \varphi_2)$ is a smooth function of the angles and equation (19) possesses one or two solutions at different θ_1 and φ_1 , while the intervals of the angles φ_2 , over which roots are available, are sufficiently large [2]. Unlike this case, the functions having alternating sign Δ_{λ_2} for the SFF and SSS mechanisms change abruptly with the angles θ_2 and φ_2 over some intervals of the angles θ_1 ($\varphi_1 = 0, \pi/4$). The number of roots of equation (19) is much larger than unity, while the intervals of the angles φ_2 , over which some of the roots are available, are narrow. At $\varphi_2 = \pi/4$ and $\theta_2 = \theta_{111}$ the function $\Delta_{t_2}(\theta_1, \varphi_1, \theta_2, \varphi_2)$ has a finite discontinuity related to the point of intersection between the spectra of quasi-transverse modes, while the function $\frac{dF(x, \varphi_2, \theta_1, \varphi_1)}{dx}$ has an infinite discontinuity at this point. In these circumstances the numerical integration of (20) using the root calculation procedure gives the function $\alpha_{\text{SSS}}^{t_2}(\theta_1, \varphi_1)$ as a ‘comb’ over some intervals of the angles θ_1 . Therefore, the introduction of a small, but finite, damping of the phonon states for the SSS mechanism is a necessary procedure. In ideal crystals the damping of phonon states is due to anharmonic scattering processes. According to experimental studies [23–25], anharmonic processes make the dominant contribution to the ultrasound absorption at $T > 10$ K. When $T \sim 100$ K and $\omega \sim 1$ GHz, the parameter $\omega_q^\lambda \tau_2 \approx 1$, while at higher temperatures the Landau–Rumer regime $\omega_q^\lambda \tau_2 < 1$ is replaced by the Akhiezer regime $\omega_q^\lambda \tau_2 > 1$ [26]. In this case, the frequency and temperature dependences of the ultrasound absorptions change qualitatively. The estimates made from measurements of the ultrasound absorptions [15–17] show that in the anharmonic scattering regime the values of the parameter $(\omega_q^\lambda \tau_2)^{-1}$ fall within the interval of 10^{-3} – 10^{-1} . Therefore, the physically reasonable limit of the parameter $\varepsilon \approx (\omega_q^\lambda \tau_2)^{-1}$ for the SSS and SFF mechanisms is 10^{-6} . The values of $\alpha_{\text{SFF}}^{t_2}(\theta_1, \varphi_1)$ calculated in this variant for the SFF mechanism agree with those calculated by formulae (17) and (18) to within the error, which is not over 1% for the SFF mechanism; the maximum error is not over 10% for the SSS mechanism. An exception to this rule is the [001] direction for the scattering of collinear phonons. In this case, the square of the matrix element (11) identically becomes zero. Therefore, if the energy conservation law is fulfilled exactly, the absorptions $\alpha_{\text{SSS}}^{t_2}(0, 0)$ and $\alpha_{\text{SFF}}^{t_2}(0, 0)$ turn to zero provided solutions corresponding to the interaction of noncollinear phonons are unavailable. However, the consideration of the small, but finite, damping leads to negligibly small, but finite, values of these quantities because of the small-angle scattering of phonons. In what follows we shall discuss the role of the interaction between collinear and noncollinear phonons in the ultrasound absorption as applied to each of the crystals studied.

Before analyzing the angular dependences of the relaxation, some comments should be made with respect to polarization vectors of quasi-transverse modes in cubic crystals. The point is that formulae (6) define components

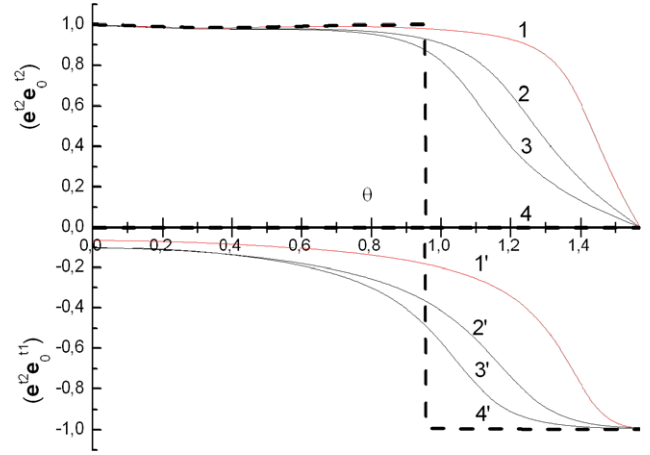


Figure 4. Angular dependences of the values $(\mathbf{e}^{t_2} \mathbf{e}_0^{t_2})$ and $(\mathbf{e}^{t_2} \mathbf{e}_0^{t_1})$ for the slow mode in the Ge crystals for the angles $\varphi = \pi/16$ —curve (1), $\varphi = \pi/8$ —(2), $\varphi = \pi/6$ —(3), $\varphi = \pi/4 - 0.01$ (4).

of the polarization vectors to the sign. Over certain variation intervals of the angles θ and φ (this interval is $\pi/4$ for the angle φ) all components of the polarization vectors simultaneously reverse sign. As can be seen from expression (13), the matrix element for the relaxation processes (1) and (2) only includes quadratic combinations of the polarization vectors \mathbf{e}_2 and, for this reason, the sign reversal will not influence the matrix element. The maximum values of longitudinal components in the quasi-transverse modes are not over 17% in Ge, GaSb, InSb and GaAs crystals and 27% in KCl. However, the angular dependences of the components in the polarization vectors \mathbf{e}^{t_1} and \mathbf{e}^{t_2} of quasi-transverse modes and their corresponding pure modes $\mathbf{e}_0^{t_1}$ and $\mathbf{e}_0^{t_2}$ differ more considerably. This is illustrated in figure 4 by the angular dependences of $(\mathbf{e}^{t_2} \mathbf{e}_0^{t_2})$ and $(\mathbf{e}^{t_2} \mathbf{e}_0^{t_1})$ characterizing the deviation of polarization vectors in a cubic crystal from polarization vectors of pure modes. It is seen from figure 4 that in the crystals of the first type the polarization vector of the slow mode \mathbf{e}^{t_2} at $\theta \rightarrow 0$ tends to the vector $\mathbf{e}_0^{t_2}$ lying in the plane $\varphi = \text{const}$; as the angle θ increases, it leaves this plane and at $\theta \rightarrow \pi/2$ it tends to the vector $\mathbf{e}_0^{t_1}$, i.e. to the direction perpendicular to the plane $\varphi = \text{const}$. Therefore, at $0 < \theta_1 < \theta_{111}$ the value of $(\mathbf{e}^{t_2} \mathbf{e}_0^{t_2})$ differs little from unity. Still, at the angles $\theta_{111} < \theta_1 < \pi/2$ the error of replacing \mathbf{e}^{t_2} by $\mathbf{e}_0^{t_2}$ reaches 100%. The polarization vector of the fast quasi-transverse mode \mathbf{e}^{t_1} exhibits a similar behavior: when $\theta \rightarrow 0$, it tends to the vector $\mathbf{e}_0^{t_1}$, i.e. to the direction perpendicular to the plane $\varphi = \text{const}$. As the angle θ increases, the vector deviates from the vector $\mathbf{e}_0^{t_1}$ and at $\theta \rightarrow \pi/2$ it tends to the vector $\mathbf{e}_0^{t_2}$, i.e. passes to the plane $\varphi = \text{const}$ (see [19], figure 4). The closer the angle φ approaches $\pi/4$, the more abruptly the angular dependences of the polarization vectors change in the vicinity of the angle $\theta = \theta_{111}$ (see figure 4). For the wavevectors lying in the diagonal plane ($\varphi_1 = \pi/4$) in the crystals of the first type the slow mode t_2 at the angles $0 < \theta_1 < \theta_{111}$ and $\pi - \theta_{111} < \theta_1 < \pi$ is a quasi-transverse mode with the polarization vector $\mathbf{e}_{q_1}^{t_2}$ lying in the diagonal plane, while at the angles $\theta_{111} < \theta_1 < \pi - \theta_{111}$ it is a pure mode with the polarization vector perpendicular to the diagonal plane ($\mathbf{e}_{q_1}^{t_2} = (-1/\sqrt{2}, 1/\sqrt{2}, 0)$). The situation

Table 2. Parameters determined for quasi-transverse ultrasound absorption for SSS and SFF relaxation mechanisms in the crystals under study.

	$A_{0TTT}^{i2} \times 10^5$ (db K ⁻⁵ cm ³ dyn ⁻²) [001]	$A_{SFF}^{i2}(\theta_1, \varphi_1) \times 10^5$ (db (cm K ⁻⁵) ⁻¹)			$A_{SSS}^{i2}(\theta_1, \varphi_1) \times 10^5$ (db (cm K ⁻⁵) ⁻¹)		
		[001]	[101]	[111]	[001]	[101]	[111]
Ge	7.59	0.003	1.94	3.06	2.832	12.49	3.52
Si	0.62	2.8×10^{-4}	0.199	0.27	0.32	0.002	0.31
Diamond	7.1×10^{-5}	1.4×10^{-6}	5.4×10^{-4}	6.3×10^{-4}	4.6×10^{-5}	0	6.97×10^{-4}
InSb	480.6	0.13	58.5	109.97	92.74	454.07	92.3
KCl	1.5×10^5	26.9	39.97	563.8	46.2	136.86	603.4
NaCl	5.4×10^3	0.14	15.8	75.6	0.59	5.16	69.1

is reverse in the crystals of the second type [19]. Therefore, the use of the pure mode approximation [15–17] can lead to large errors in the angular dependences of the relaxation rates for the TTT mechanisms. We shall show below that the behavior of the polarization vectors, which is noted in [19], causes the appearance of special features in the angular dependences of the relaxation rates for the TTT mechanisms in directions like [111].

3. Results of the numerical analysis

From formulae (9)–(15) and (19)–(21) it is possible to calculate the absorption $A_{TTT}^{i2}(\theta_1, \varphi_1)$ characterizing the dependence of the ultrasound absorption on the direction of the sound wavevector for the TTT mechanisms. We shall compare the contributions from the SSS and SFF mechanisms and the contribution from the Landau–Rumer mechanism [2], and find the full absorption of quasi-transverse ultrasound of the ST mode:

$$\alpha_{t_2}(z_1, T, \theta_1, \varphi_1) = \alpha_{SSS}^{i2} + \alpha_{SFF}^{i2} + \alpha_{TLL}^{i2} \\ = A_{t_2}(\theta_1, \varphi_1) z_1 T^5 (\text{dB cm}^{-1}), \quad (22)$$

$$A_{t_2}(\theta_1, \varphi_1) = A_{SSS}^{i2}(\theta_1, \varphi_1) + A_{SFF}^{i2}(\theta_1, \varphi_1) + A_{TLL}^{i2}(\theta_1, \varphi_1) \\ = A_{0TTT}^{i2} (J_{SSS}^{i2}(\theta_1, \varphi_1) + J_{SFF}^{i2}(\theta_1, \varphi_1)) \\ + A_{0TLL} J_{TLL}^{i2}(\theta_1, \varphi_1). \quad (23)$$

$$A_{0TLL}^{i2} = \frac{4.34\pi^3 k_B^5}{15\hbar^4 \rho^3 (S_{t_2}(\theta_1, \varphi_1))^2 \langle S_L \rangle^8},$$

$$A_{0TTT}^{i2}/A_{0TLL}^{i2} = \frac{\langle S_L \rangle^8}{(S_{100}^{i2})^8} \approx \left(\frac{c_{11}}{c_{44}} \right)^4.$$

The quantity $A_{t_2}(\theta_1, \varphi_1)$ characterizes the anisotropy of the full absorption of the mode t_2 . The corresponding dependences are calculated for the two most important cases, when the phonon wavevectors lie in the planes of the cube faces or the diagonal planes. The calculations are made using experimental values of thermodynamic elastic moduli of the second c_{ij} and the third c_{ijk} order adopted from [4, 27] (see table 1).

Figures 5 present the absorption of quasi-transverse ultrasound in cubic crystals of Ge, Si and InSb for the SSS and SFF mechanisms in the pure mode approximation as calculated by formulae (17) (curves 1' and 2') and taking exactly into account the polarization vectors (curves 1 and 2). In the [001] and [101] directions the roughly calculated values of

$\alpha_{SSS}^{i2}(\theta_1, \varphi_1)$ and $\alpha_{SFF}^{i2}(\theta_1, \varphi_1)$ for the wavevectors of phonons in the planes of the cube faces differ from those calculated exactly by less than 2.5 times. For example, this relationship for $\alpha_{SSS}^{i2}(\theta_1, \varphi_1)$ is 2.4, 2.5 and 1.8 in directions like [001] and 2.1, 1.1 and 1.4 in directions like [101] for Ge, Si and InSb crystals respectively. However, the comparison of curves 1, 2 and 1', 2' shows that the pure mode approximation does not provide the correct description of the angular dependences of the absorption of quasi-transverse modes via the SSS and SFF mechanisms in cubic crystals. It disturbs the cubic symmetry for the absorption: in the [001] and [100] directions the values of $\alpha_{SSS}^{i2}(\theta_1, \varphi_1)$ and $\alpha_{SFF}^{i2}(\theta_1, \varphi_1)$ coincide (curves 1 and 2) when the polarization vectors are taken into account exactly, whereas they differ by nearly one order of magnitude when the pure mode approximation is used. Thus, this approximation is not correct for the quantitative description of the anisotropy of ultrasound absorption in cubic crystals.

Analyzing the calculation results, we shall note, in the first place, some characteristic features determining the efficiency of the relaxation mechanisms at hand in the crystals under study. Firstly, in all the crystals studied, except diamond, the total contribution of the SSS and SFF relaxation mechanisms to the absorption is considerably larger than the contribution from the Landau–Rumer mechanism: several times or one to two orders of magnitude depending on the direction (see figures 5–8). The dominance of the SSS and SFF relaxation mechanisms over the Landau–Rumer mechanism is due in large measure to the second-order elastic moduli. As is clear from (23) the ratio of A_{0TTT}^{i2} and A_{0TLL}^{i2} in the TTT and Landau–Rumer relaxation mechanisms is proportional to $(c_{11}/c_{44})^4$, which is much larger than unity. This ratio is 26, 32, 16 and 48 for the crystals of the first group (Ge, Si, diamond and InSb respectively). Notice that the coefficient A_{0TTT}^{i2} is 715 and 154 times higher than A_{0TLL}^{i2} in the ionic KCl and NaCl crystals respectively. Such a large excess of A_{0TTT}^{i2} over A_{0TLL}^{i2} , which characterizes the absorption via the Landau–Rumer mechanism, in the KCl crystal is due to anomalously small values of the second-order elastic moduli c_{ik} determining the propagation rate of transverse phonons (see table 1). In the crystals of the first type the absorptions $\alpha_{SSS}^{i2}(\theta_1, \varphi_1)$ and $\alpha_{SFF}^{i2}(\theta_1, \varphi_1)$ decrease in directions like [001] nearly by one order of magnitude in going from Ge to Si and two orders of magnitude in going from Si to diamond. This decrease is due mainly to the change of the coefficient A_{0TTT}^{i2} , which depends on the second-order elastic moduli (see table 2). The coefficient A_{0TTT}^{i2} decreases

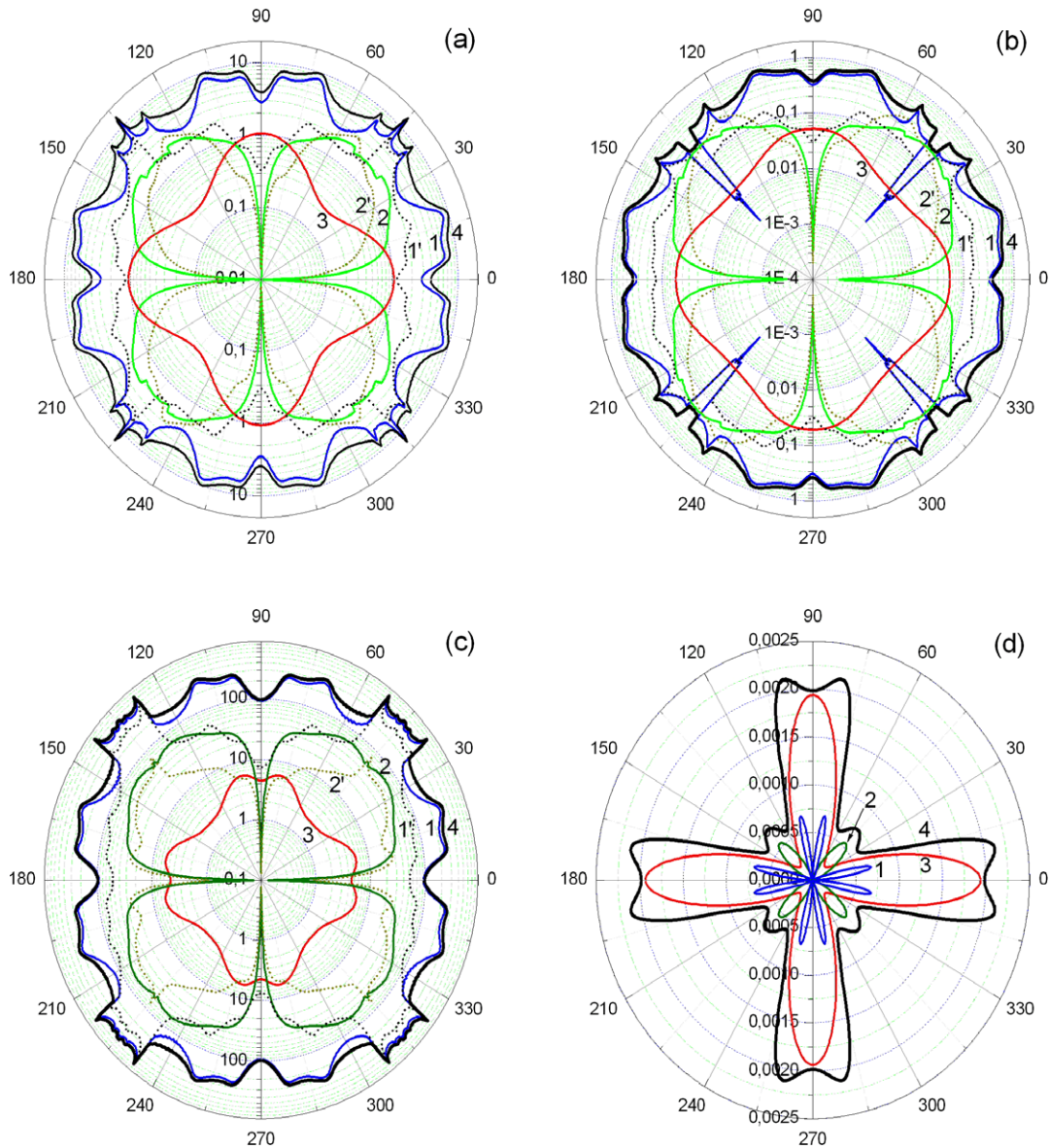


Figure 5. Angular dependences of the absorptions of the slow quasi-transverse mode in Ge (a), Si (b), InSb (c) and diamond (d) crystals with wavevectors in the cube face plane: the SSS relaxation mechanism (curve 1), the SFF relaxation mechanism (curve 2), the Landau–Rumer mechanism (curve 3), and the full quasi-transverse ultrasound absorption (curve 4). The dashed curves 1' and 2' denote the absorptions in Ge, Si and InSb crystals as calculated in the pure mode approximation from formulae (17) for the SSS and SFF mechanisms respectively.

by one order of magnitude in going from Ge to Si and four orders of magnitude in going from Si to diamond. However, in diamond crystals the two orders of magnitude of the absorption coefficient are compensated by large values of the third-order elastic moduli, which determine the probability of anharmonic scattering processes (see table 1).

Secondly, in Ge, Si, InSb and KCl, which are crystals with a significant anisotropy of the elastic energy, the SSS mechanism is more efficient than the SFF mechanism (see Table 2). It largely determines the total absorption of the slow quasi-transverse mode in Ge, Si, InSb and KCl. The dominance of the SSS relaxation mechanism over SFF is explained by the fact that the denominator of the integral $J_{SSS}^2(\theta_1, \varphi_1)$ includes the phase velocity of the slow mode $S_{r2}(\theta_2, \varphi_2)$ to the eighth power, whereas $J_{SFF}^2(\theta_1, \varphi_1)$ includes

the phase velocity of the fast mode $S_{r1}(\theta_2, \varphi_2)$ to the eighth power (see formula (11)), with $S_{r2}(\theta_2, \varphi_2) \leq S_{r1}(\theta_2, \varphi_2)$. Table 4 gives the ratios of the average velocities of the fast and slow modes to the eighth power for all the crystals under study. For example, this ratio is six in KCl.

Thirdly, the angular dependences of the absorption of the slow quasi-transverse mode in the cubic crystals of the first type ($\Delta C > 0$, Ge, Si, diamond and InSb) are qualitatively different for the TTT and Landau–Rumer relaxation mechanisms (see figures 5). In the crystals of the first type (Ge, Si, diamond and InSb) the maximum values of the absorption $\alpha_{TLL}^2(\theta_1, \varphi_1)$ are reached in crystallographic directions like [001] (Ge, Si and diamond) or directions close to [001] (InSb), whereas its minimum values are reached in directions like [101] and [111]. Oppositely, in the case

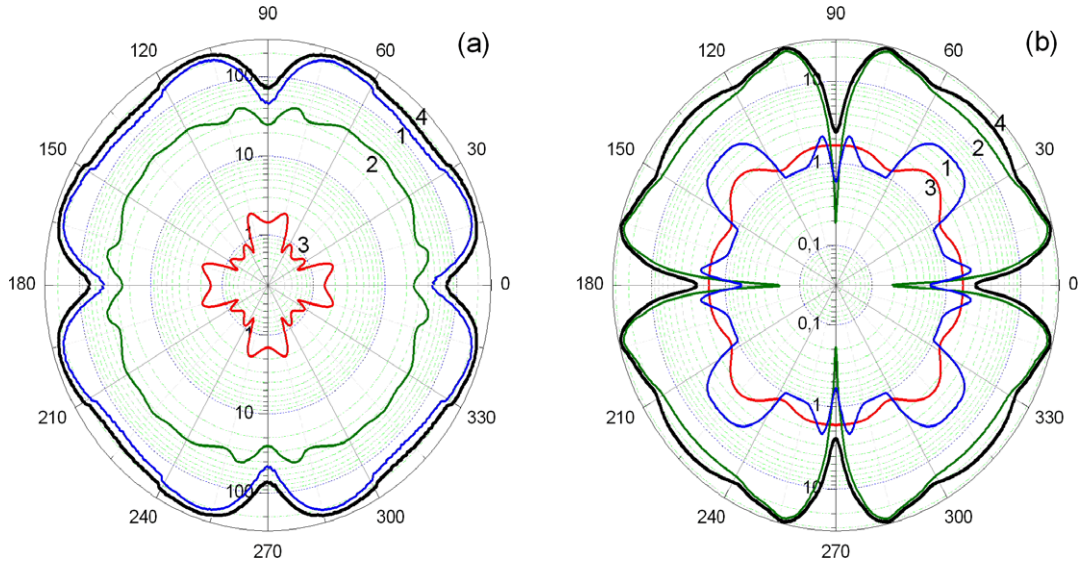


Figure 6. Angular dependences of the absorption of the slow quasi-transverse mode in the KCl (a) and NaCl (b) crystals with the wavevector in the cube face plane: the SSS relaxation mechanism (curve 1), the SFF relaxation mechanism (curve 2), the Landau–Rumer mechanism (curve 3) and full quasi-transverse ultrasound absorption (curve 4).

of the TTT relaxation mechanism the minimum values of the absorptions $\alpha_{\text{SSS}}^{t_2}(\theta_1, \varphi_1)$ and $\alpha_{\text{SFF}}^{t_2}(\theta_1, \varphi_1)$ are reached in directions like [001], while their maximum values are realized in crystallographic directions like [101] and [111] or directions close to them. Thus, the angular dependences of the absorptions via the TTT and Landau–Rumer relaxation mechanisms in the crystals of the first type are reversed. The SSS relaxation mechanism makes the dominant contribution to the absorption in all directions of the wavevector in KCl crystals. It is several times larger than the contribution from the SFF relaxation mechanism and two orders of magnitude larger than that from the Landau–Rumer mechanism. By contrast, in NaCl crystals the contribution from the Landau–Rumer mechanism dominates in the [001] directions, while over a large interval of angles the full absorption is determined by the total contribution from the SFF and SSS relaxation mechanisms.

Let us discuss in more detail the anisotropy of the absorption of the slow quasi-transverse mode t_2 when the wavevectors \mathbf{q}_1 and the polarization vectors of the sound wave lie in the cube face plane ($\varphi_1 = 0$) (see figures 5 and 6). It is seen from these figures that with the dominant role of anharmonic scattering processes the consideration of one of the TTT or Landau–Rumer relaxation mechanisms is insufficient for the quantitative description of the anisotropy of relaxation rates in the cubic crystals. For example, the contributions of the SSS, SFF and Landau–Rumer mechanisms to the full absorption in directions of the [001] type in the crystals of the first type are 72.6%, 0.1% and 27.3% in Ge, 86.4%, 0.1% and 13.5% in Si, and 95.3%, 0.1% and 4.6% in InSb respectively. It follows from the solution to equation (19) that in directions of the [001] type the SFF relaxation mechanism can only involve collinear phonons ($\theta_{12} = 0$). In this case, the square of the matrix element (15) identically turns to zero (see figure 1(a)). Therefore, if the energy conservation law is

fulfilled exactly, the absorption of the quasi-transverse mode $\alpha_{\text{SFF}}^{t_2}(0, 0)$ turns to zero. However, the consideration of the small, but finite, damping ($\varepsilon = 10^{-6}$) leads to a negligibly small, but finite, value of $\alpha_{\text{SFF}}^{t_2}(0, 0)$. For the SSS relaxation mechanism the energy conservation law allows the interaction of both collinear and noncollinear phonons in directions like [001] (see figure 3(a)). The contribution from the interaction of collinear phonons to the absorption is negligibly small. In the case of noncollinear phonons the integral $J_{\text{SSS}}^{t_2}(0, 0)$ in Ge crystals is 9.8 times smaller than the corresponding integral $J_{\text{TLL}}^{t_2}(0, 0)$ for the Landau–Rumer mechanism, but the coefficient $A_{\text{TTT}}^{t_2}$ is 26 times larger than $A_{\text{OTLL}}^{t_2}$. Therefore the absorption $\alpha_{\text{SSS}}^{t_2}(0, 0)$ is almost three times larger than it is via the Landau–Rumer mechanism. In Ge, Si and InSb crystals the absorption $\alpha_{\text{TLL}}^{t_2}(\theta_1, 0)$ is the minimum in directions like [101] ($\theta_1 = \pi/4$), while the dominant contribution to the full absorption is made by the TTT relaxation mechanisms, which change qualitatively the angular dependences $\alpha_{t_2}(\theta_1, 0)$ as compared to those in the Landau–Rumer mechanism. In these directions the full absorption reaches the maximum in Ge crystals, a local maximum in InSb crystals, and the minimum in Si (see figures 5(a), (b) and (c), curves 4). The contributions from the SSS, SFF and Landau–Rumer relaxation mechanisms to the full absorption are 85.2%, 13.2% and 1.6% in Ge, 0.9%, 90%, and 9.1% in Si and 88.3%, 11.3% and 0.4% in InSb respectively. The considerable change in the contributions from the SSS and SFF relaxation mechanisms in going from Ge to Si crystals is due to the decrease in the cubic anisotropy, namely the parameter $k - 1$ (see table 1). It is seen from figure 3(b) that the solutions to equation (19), which correspond to the scattering to large angles in Ge crystals, are absent for Si crystals and the range of other roots for Si is narrow. Therefore the value of the integral $J_{\text{SSS}}^{t_2}(\pi/4, 0)$ in Si becomes four orders of magnitude smaller than it is in Ge. While the coefficient $A_{\text{TTT}}^{t_2}$ is 32 times larger than $A_{\text{OTLL}}^{t_2}$

in Si, the value of $\alpha_{\text{SSS}}^{t_2}(\pi/4, 0)$ proves to be two orders of magnitude smaller than $\alpha_{\text{TLL}}^{t_2}(\pi/4, 0)$ (see figure 5(b), curves 1 and 3). On the other hand, the range of the roots for equation (19) corresponding to the interaction of noncollinear phonons is much wider for the SFF relaxation mechanism. Therefore, the SFF relaxation mechanism dominates in Si and its contribution is ten times larger than the contribution from the Landau–Rumer mechanism. The ratio between the values of $\alpha_{t_2}(\pi/4, 0)$ and $\alpha_{t_2}(0, 0)$ corresponding to the [001] directions is 3.8, 0.6 and 5.3 in Ge, Si and InSb respectively. The maximum values of the full absorption $\alpha_{t_2}(\theta_1, 0)$ in InSb crystals are reached in directions close to [101] at $\theta_1 = \pi/4 \pm 0.13$ and are seven times larger than $\alpha_{t_2}(0, 0)$.

The cubic anisotropy parameter $k - 1$ is much smaller in diamond than it is in Ge and InSb crystals and, hence, the TTT relaxation mechanisms are less significant for diamond. The full absorption $\alpha_{t_2}(\theta_1, 0)$ is determined to a large extent by the Landau–Rumer mechanism. The consideration of the SSS and SFF relaxation mechanisms gives rise to additional features in the dependence of $\alpha_{t_2}(\theta_1, 0)$ on the angle θ_1 (see figure 5(d), curves 1, 2 and 4). The Landau–Rumer mechanism makes the dominant contribution to the ultrasound absorption in the [001] directions. The solution to equation (19) for these directions suggests that the SSS and SFF relaxation mechanisms can only involve collinear phonons ($\theta_{12} = 0$). Therefore, if the energy conservation law is fulfilled exactly, the absorptions $\alpha_{\text{SSS}}^{t_2}(0, 0)$ and $\alpha_{\text{SFF}}^{t_2}(0, 0)$ turn to zero. However, the consideration of the small, but finite, damping leads to negligibly small, but finite, values of these quantities because of the small-angle scattering. As a result, in the [001] directions at $\varepsilon = 10^{-6}$ the contribution of the Landau–Rumer mechanism to the full absorption is 40 times larger than the total contribution from the SSS and SFF relaxation mechanisms. The full absorption in this direction $\alpha_{t_2}(0, 0)$ has a local minimum because the absorption via the SSS mechanism reaches its maximum values in directions close to [001] ($\theta_1 \cong \pi/2n \pm 0.2$). These maxima are due to the interaction of noncollinear phonons. They are 2.8 times smaller than $\alpha_{\text{TLL}}^{t_2}(0, 0)$, but lead to the formation of maxima in the full absorption $\alpha_{t_2}(\theta_1, 0)$ at the angles $\theta_1 \cong \pi/2n \pm 0.16$. The maxima are a factor of 1.1 larger than the value of $\alpha_{t_2}(0, 0)$. At the angles $\pi/6 < \theta_1 < \pi/3$ equation (19) does not possess a solution for the SSS mechanism and $\alpha_{\text{SSS}}^{t_2}(\theta_1, 0)$ is zero (see figure 5(d), curves 1). The SFF mechanism dominates over this interval. The ultrasound absorption for this mechanism reaches its maximum values in directions like [101] and causes the formation of a local maximum in the dependence of the full absorption $\alpha_{t_2}(\theta_1, 0)$. The value of $\alpha_{t_2}(\pi/4, 0)$ proves to be 2.6 times smaller than that of $\alpha_{t_2}(0, 0)$. The function $\alpha_{t_2}(\theta_1, 0)$ in diamond reaches its equal minimum values at the angles $\theta_1 \cong \pi/6$ and $\theta_1 \cong \pi/3$ and these minimum values are 3.2 times smaller than the values of $\alpha_{t_2}(0, 0)$. A strong dependence of the ultrasound absorption $\alpha_{\text{SSS}}^{t_2}(\theta_1, 0)$ in directions of the [101] type on the parameter $k - 1$ is noteworthy in Ge, Si and diamond crystals. In Ge the parameter $k - 1 = 0.87$ and the absorption $\alpha_{\text{SSS}}^{t_2}(\pi/4, 0)$ has a maximum, which is 52 times larger than $\alpha_{\text{TLL}}^{t_2}(\pi/4, 0)$. In Si the parameter $k - 1 = 0.67$ and the absorption $\alpha_{\text{SSS}}^{t_2}(\pi/4, 0)$ has a deep minimum, while $\alpha_{\text{SSS}}^{t_2}(\pi/4, 0)$ is 10 times smaller

Table 3. Parameters determined for quasi-transverse ultrasound absorption for Landau–Rumer relaxation mechanism in the crystals under study [2].

	$A_{\text{TLL}}^{t_2} \times 10^5$ (db K ⁻⁵ cm ³ dyn ⁻²)	$A_{\text{TLL}}^{t_2}(\theta_1, \varphi_1) \times 10^5$ (db (cm K ⁻⁵) ⁻¹)		
		[001]	[101]	[111]
Ge	0.29	1.06	0.24	0.34
Si	0.019	0.05	0.02	0.02
Diamond	4.4×10^{-6}	0.0019	2×10^{-4}	5.8×10^{-4}
InSb	9.91	4.49	2.12	1.71
KCl	210	1.44	0.68	133.6
NaCl	34.7	1.67	2.34	41.4

than $\alpha_{\text{TLL}}^{t_2}(\pi/4, 0)$. In diamond the parameter $k - 1 = 0.4$ and the absorption $\alpha_{\text{SSS}}^{t_2}(\pi/4, 0) = 0$.

In the cubic KCl and NaCl crystals with a negative anisotropy of the second-order elastic moduli the ratio of the contributions from the SSS and SFF relaxation mechanisms to the ultrasound absorption is considerably different. The KCl crystals are most anisotropic among the crystals of the second group. The relaxation rates $\alpha_{\text{SSS}}^{t_2}(0, 0)$ and $\alpha_{\text{SFF}}^{t_2}(0, 0)$ in these crystals are due to the interaction of noncollinear phonons, while the dominant contribution to the full absorption $\alpha_{t_2}(\theta_1, 0)$ is made by the SSS mechanism. The contributions of the SSS, SFF and Landau–Rumer relaxation mechanisms to the full ultrasound absorption are 62%, 36% and 2% in directions like [001], and 77%, 22.5% and 0.5% in directions like [101]. Thus, the Landau–Rumer relaxation mechanism makes a negligibly small contribution to the absorption of the slow quasi-transverse mode. In KCl the full absorption reaches its maximum values at the angles $\theta_1 \cong n\pi/2 \pm 0.35$ ($n = 0, 1, 2$, etc) and its minimum values in directions like [001]; a local minimum is realized in the [101] directions ($\theta_1 = \pi/4$) (see figure 6(a), curves 4). Oppositely, in the NaCl crystals the Landau–Rumer mechanism dominates in the [001] directions and the full absorption is determined by the SFF relaxation mechanism over a wide interval of the angles $0.12 < \theta_1 < 1.45$ (see figure 6(b), curves 2, 3 and 4). In the [001] directions the SSS and SFF relaxation mechanisms can only involve collinear phonons ($\theta_{12} = 0$). Therefore, if the energy conservation law is fulfilled exactly, the absorptions $\alpha_{\text{SSS}}^{t_2}(0, 0)$ and $\alpha_{\text{SFF}}^{t_2}(0, 0)$ turn to zero in the NaCl crystals. However, taking into account an insignificant damping, they become nonzero because of the small-angle scattering. At $\varepsilon = 10^{-6}$ the contribution from the Landau–Rumer mechanism to the full absorption is 2.3 times larger than the total contribution from the SSS and SFF relaxation mechanisms (see table 3). The absorptions $\alpha_{\text{SSS}}^{t_2}(\theta_1, 0)$ and $\alpha_{\text{TLL}}^{t_2}(\theta_1, 0)$ reach their maxima in directions like [101] ($\theta_1 = \pi/4$). For the Landau–Rumer mechanism, the absorption $\alpha_{\text{SSS}}^{t_2}(\pi/4, 0)$ is 2.2 times higher than $\alpha_{\text{TLL}}^{t_2}(\pi/4, 0)$. In the NaCl crystals the full absorption $\alpha_{t_2}(\theta_1, 0)$ reaches its maximum values at the angles $\theta_1 \cong n\pi/2 \pm 0.24$ ($n = 0, 1, 2$, etc), while a local maximum is realized in the [101] directions ($\theta_1 = \pi/4$) (see figure 6(b), curve 4). In the KCl and NaCl crystals the full ultrasound absorption $\alpha_{t_2}(\theta_1, 0)$ reaches its minimum values in directions of the [001] type (see table 3). It should be noted that the anisotropy of the full absorption

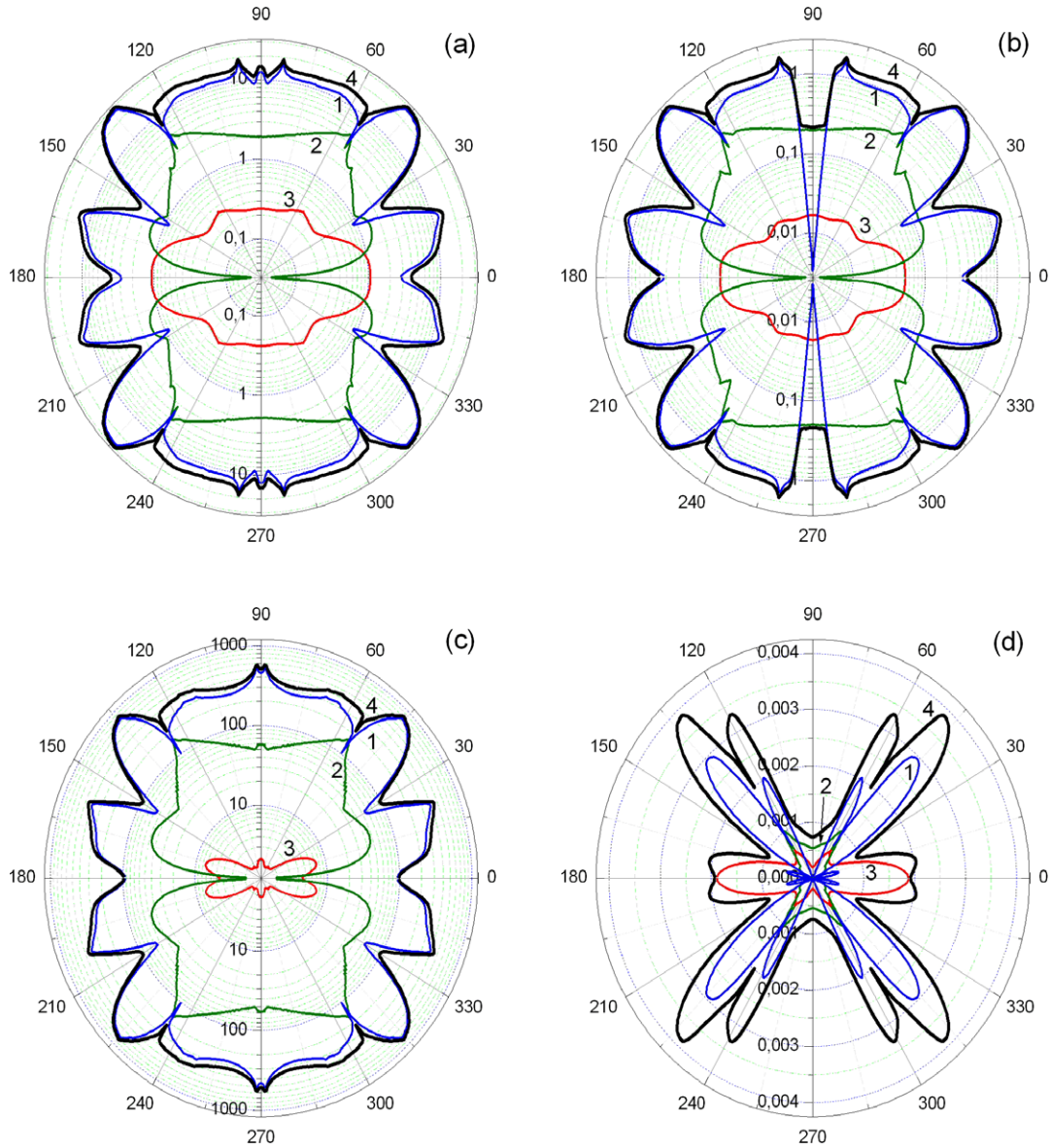


Figure 7. Angular dependences of the absorption of the slow quasi-transverse mode in the Ge (a), Si (b), InSb (c) and diamond (d) crystals with the wavevector in the diagonal plane: the SSS relaxation mechanism (curve 1), the SFF relaxation mechanism (curve 2), the Landau–Rumer mechanism (curve 3) and full quasi-transverse ultrasound absorption (curve 4).

$\alpha_{t2}(\theta_1, 0)$ is considerably different from the anisotropy of the ultrasound absorption via the Landau–Rumer mechanism. For example, the ratio of $\alpha_{t2}(\pi/4, 0)$ and $\alpha_{t2}(0, 0)$ is 2.4 and 9.7 in KCl and NaCl respectively. For the Landau–Rumer mechanism, the ratio of $\alpha_{TLL}^2(\pi/4, 0)$ and $\alpha_{TLL}^2(0, 0)$ equals 0.5 and 1.4 in KCl and NaCl respectively.

The angular dependences of the absorptions $\alpha_{SSS}^2(\theta_1, \pi/4)$, $\alpha_{SFF}^2(\theta_1, \pi/4)$ and $\alpha_{t2}(\theta_1, \pi/4)$ in the crystals of the first and second types are more complicated for sound wavevectors lying in the diagonal plane ($\varphi_1 = \pi/4$) (see figures 7 and 8). This is due to both the presence of the intersection point of the spectra of quasi-transverse modes and the behavior of the polarization vectors of the slow mode [19]. As mentioned above, in the crystals of the first type the slow mode t_2 is a quasi-transverse mode with the polarization vector lying in the diagonal plane at the angles $0 < \theta_1 < \theta_{111}$ and $\pi - \theta_{111} < \theta_1 < \pi$, while

it is a pure mode with the polarization vector perpendicular to the diagonal plane at the angles $\theta_{111} < \theta_1 < \pi - \theta_{111}$. In the crystals of the second type these intervals of the angles change places (for details see [19]). In this connection, the angular dependences of the absorptions $\alpha_{SSS}^2(\theta_1, \pi/4)$, $\alpha_{SFF}^2(\theta_1, \pi/4)$ and $\alpha_{t2}(\theta_1, \pi/4)$ in directions like [111] exhibit singularities: sharp local minima are observed in the crystals of the first type (Ge, Si, diamond and InSb) and the NaCl crystal of the second type, whereas an absolute maximum is realized in the KCl crystal for the SFF mechanism and a local minimum for the SSS relaxation mechanism.

As can be seen from figures 7(a), (b) and (c), in the case at hand ($\varphi_1 = \pi/4$) the angular dependences of the absorptions $\alpha_{SSS}^2(\theta_1, \pi/4)$, $\alpha_{SFF}^2(\theta_1, \pi/4)$ and $\alpha_{t2}(\theta_1, \pi/4)$ are qualitatively similar in the Ge, Si and InSb crystals. The SSS relaxation mechanism dominates over the whole interval of

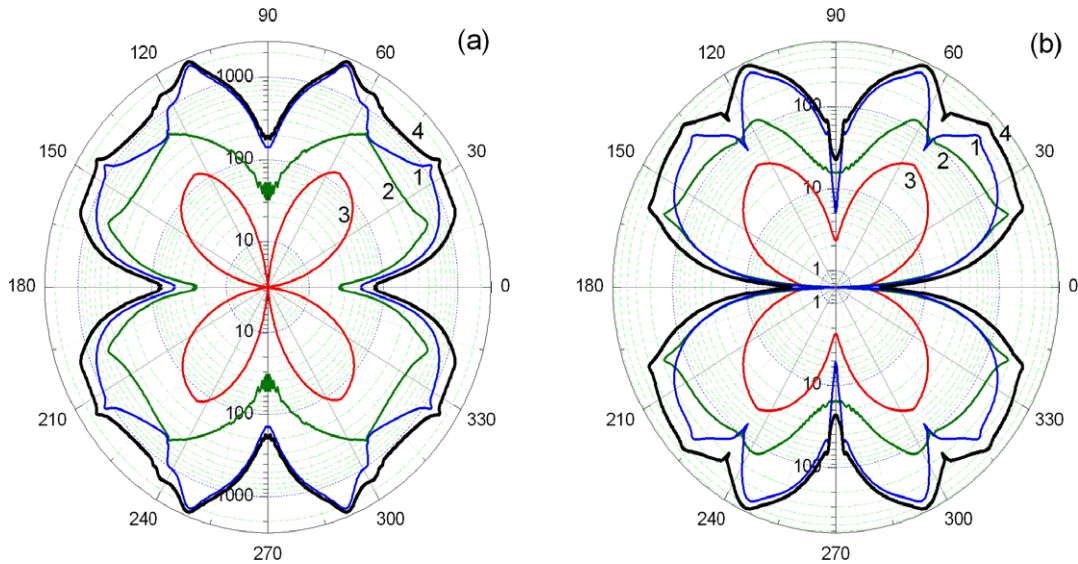


Figure 8. Angular dependences of the absorption of the slow quasi-transverse mode in the KCl (a) and NaCl (b) crystals with the wavevector in the diagonal plane: the SSS relaxation mechanism (curve 1), the SFF relaxation mechanism (curve 2), the Landau–Rumer mechanism (curve 3), and full quasi-transverse ultrasound absorption (curve 4).

Table 4. Parameters determined for full quasi-transverse ultrasound absorption in the crystals under study.

	$A_{i2}(\theta_1, \varphi_1) \times 10^5 \text{ (db (cm K}^{-5}\text{)}^{-1})$				$(\langle s_{r1} \rangle / \langle s_{r2} \rangle)^8$	A_{0TTT}^2 / A_{0TLL}^2 [001]
	[001]	[101]	[111]			
Ge	3.88	14.67	6.92	2.8	26	
Si	0.37	0.22	0.6	2.5	32	
Diamond	0.00195	7.4×10^{-4}	0.00191	1.5	16	
InSb	97.4	514.3	204	3.7	48	
KCl	74.5	177.5	1.3×10^3	5.96	715	
NaCl	2.4	23.3	186.1	2.0	154	

the angles θ_1 and the values of the absorptions $\alpha_{i2}(\theta_1, \pi/4)$ and $\alpha_{SSS}^2(\theta_1, \pi/4)$ are nearly equal (see figures 7(a), (b) and (c), curves 1 and 4). The absorptions $\alpha_{SSS}^2(\theta_1, \pi/4)$ and $\alpha_{i2}(\theta_1, \pi/4)$ are minimum in directions like [001] and [111], in directions close to [011], and at $\theta_1 \cong \pi/6$. The functions $\alpha_{i2}(\theta_1, \pi/4)$ reach their absolute minima at the angles $\theta_1 \cong \pi/6$ and these minima are 1.5, 1.8 and 1.1 times smaller than those of $\alpha_{i2}(0, \pi/4)$ in Ge, Si and InSb respectively. The contribution from the Landau–Rumer mechanism is 27%, 13% and 4.6% in directions like [001] in Ge, Si and InSb respectively. In directions like [111] the contribution from the Landau–Rumer mechanism is much smaller, while the contributions from the SSS and SFF relaxation mechanisms are approximately equal (see figures 7(a), (b) and (c), curves 1, 2 and 3). The maximum values of the full absorption $\alpha_{i2}(\theta_1, \pi/4)$ in Ge, Si and InSb are reached at angles close to $\theta_1 = \pi/4$ and they are due to the SSS relaxation mechanism. These values are 7.1, 6.2 and 8 times larger than those of $\alpha_{i2}(0, \pi/4)$ in Ge, Si and InSb respectively.

The situation with the absorptions in the diamond crystals is considerably different for the wavevectors lying in the diagonal plane ($\varphi_1 = \pi/4$) and the cube face plane ($\varphi_1 = 0$). The Landau–Rumer mechanism makes the dominant contribution to the full absorption in directions like [001]

and this contribution is the maximum in the [001] direction. However, the total relaxation rate has a local minimum in this direction. The absolute maximum of the full absorption $\alpha_{i2}(\theta_1, \pi/4)$ is realized at the angles $\theta_1 \cong \pi/4$ and is due to the SSS relaxation mechanism. It is nearly twice as large as the corresponding value for $\alpha_{i2}(0, \pi/4)$. At the angles $\pi/2.6 < \theta_1 < \pi/2$ the contribution from the SSS relaxation mechanism turns to zero and the SFF mechanism dominates (see figures 7(d), curves 1 and 2). The absorption via the SFF mechanism reaches its maximum values in directions close to [111]. In directions like [110] ($\theta_1 \cong \pi/2$) the full absorption $\alpha_{i2}(\theta_1, \pi/4)$ reaches its minimum value and the contribution from the SFF mechanism is 2.7 times larger than the contribution from the Landau–Rumer mechanism. In diamond the function $\alpha_{i2}(\theta_1, \pi/4)$ has a local maximum at $\theta_1 \cong 1.07$ and three local minima at $\theta_1 \cong \pi/2$, $\theta_1 = \theta_{111}$ and $\theta_1 \cong 0.43$.

In the KCl and NaCl crystals the absorption anisotropy for the wavevectors lying in the diagonal plane ($\varphi_1 = \pi/4$) is much larger than that for the wavevectors in the cube face plane (see figures 8, curves 4). In these crystals the full absorption reaches its minimum values in directions like [001] ($\theta_1 = 0$). In the KCl crystals the values of $\alpha_{i2}(0, \pi/4)$ depend on the total contribution from the SSS and SFF relaxation

mechanisms, whereas in the NaCl crystals they are determined by the Landau–Rumer mechanism. The absolute maxima of the full absorption $\alpha_{t2}(\theta_1, \pi/4)$ are due to the SSS relaxation mechanism and are realized at the angles $\theta_1 \cong 1.2$ and 1.15 in the KCl and NaCl crystals respectively. They are 33 and 240 times larger than the minimum values of $\alpha_{t2}(0, \pi/4)$ in KCl and NaCl respectively. Moreover, in the KCl crystals the function $\alpha_{t2}(\theta_1, \pi/4)$ has local maxima at the angles $\theta_1 = \theta_{111}$ and $\theta_1 \cong 0.6$ and these maxima are 21 and 22 times larger than those of $\alpha_{t2}(0, 0)$. The first maximum results from the SFF relaxation mechanism, while the second maximum is due to the SSS relaxation mechanism. As distinct from KCl, in the NaCl crystals the full absorption $\alpha_{t2}(\theta_1, \pi/4)$ in directions like [111] and the values of $\alpha_{SSS}^{t2}(\theta_1, \pi/4)$ and $\alpha_{SFF}^{t2}(\theta_1, \pi/4)$ have sharp local minima, similarly to the crystals of the first group (see figure 8(b), curves 1, 2 and 4). The value of $\alpha_{t2}(\theta_{111}, \pi/4)$ is 78 times larger than the minimum values of $\alpha_{t2}(0, \pi/4)$ in directions like [001]. The contributions from the SSS, SFF and Landau–Rumer mechanisms to the full absorptions in directions like [111] are 47%, 43% and 10% in the KCl crystals and 37%, 41% and 22% in the NaCl crystals.

Thus, the absorptions are the maximum in the KCl and InSb crystals among those studied: the coefficient $A_{t2}(\theta_1, \pi/4)$ is as high as 2520 (dB cm⁻¹ K⁻⁵) at the angles $\theta_1 \cong 1.19$ in KCl and 820 (dB cm⁻¹ K⁻⁵) at the angles $\theta_1 \cong \pi/4$ in InSb. The absorptions are the minimum in the diamond crystals: coefficient $A_{t2}(\theta_1, 0) = 0.0006$ (dB cm⁻¹ K⁻⁵) at θ_1 equal to $\pi/6$ and $\pi/3$.

4. Conclusion

The absorption of quasi-transverse ultrasound during anharmonic scattering processes in cubic crystals with a positive (Ge, Si, diamond and InSb) and a negative (KCl and NaCl) anisotropy of the second-order elastic moduli was studied. The absorption of slow quasi-transverse modes via the SSS, SFF and Landau–Rumer relaxation mechanisms was discussed. The angular dependences of the absorptions of the slow quasi-transverse modes for the SSS and SFF relaxation mechanisms were analyzed in the context of the anisotropic continuum model and the full absorptions were determined. Two most important cases when the wavevectors of phonons are in the planes of the cube faces or in the diagonal planes were considered. It was shown that the pure mode approximation cannot be adequately used for the quantitative description of the ultrasound absorption anisotropy in cubic crystals. The main results of the study can be formulated as follows:

- (1) The absorptions of quasi-transverse ultrasound in cubic crystals are calculated for the SSS and SFF relaxation mechanisms in a long-wavelength approximation. It is shown that in crystals with a considerable anisotropy of the elastic energy (Ge, Si, InSb, KCl and NaCl) the total contribution from the SSS and SFF relaxation mechanisms to the ultrasound absorption is several times or one to two orders of magnitude larger than the contribution from the Landau–Rumer mechanism depending on the direction. The dominance of the SSS and SFF relaxation mechanisms over the Landau–Rumer

mechanism is explained, to a large extent, by the second-order elastic moduli. The role of the Landau–Rumer mechanism in the ultrasound absorption is considerable in diamond crystals with a smaller anisotropy of the elastic energy.

- (2) The full absorptions of slow quasi-transverse modes are determined. Other variants of the ST mode relaxation, except the ones considered above, leading to the dependence of the Landau–Rumer type are unavailable. It is shown that with the anharmonic scattering processes playing the dominant role, the consideration of one of the relaxation mechanisms—the Landau–Rumer mechanism or the SSS or SFF mechanism—is insufficient for describing the anisotropy of the full ultrasound absorption in cubic crystals.
- (3) In Ge, Si, InSb and KCl crystals the contribution from the SSS mechanism is times or orders of magnitude larger than the contribution from the SFF mechanism. In diamond and NaCl crystals the two contributions are of the same order of magnitude. The dominance of the SSS mechanism over SFF is due mainly to the second-order elastic anisotropy, i.e. the relation between the second-order elastic moduli.
- (4) It is shown that the SSS and SFF relaxation mechanisms are due to the cubic anisotropy of the crystals leading to the interaction of noncollinear phonons.
- (5) The analysis of three-phonon scattering processes via the SSS and SFF relaxation mechanisms in cubic crystals demonstrated that the square of the matrix element turns to zero during the scattering of collinear phonons when the slow ST mode is a purely transverse mode and is nonzero when the slow ST mode is quasi-transverse. The behavior of the square of the matrix element during the scattering of collinear phonons is qualitatively different in the crystals of the first and second groups.
- (6) It is found that the presence of intersection points of the spectra of quasi-transverse modes and a sharp change of the polarization vectors near the [111] directions give rise to strong singularities in the absorptions of quasi-transverse ultrasound in the vicinity of these directions.
- (7) The SSS and SFF relaxation mechanisms can involve collinear phonons in directions like [001]. However, in this case the square of the matrix element identically turns to zero as in the isotropic medium model. Therefore the absorptions of the slow quasi-transverse mode, $\alpha_{SSS}^{t2}(0, 0)$ and $\alpha_{SFF}^{t2}(0, 0)$, become zero if the energy conservation law is fulfilled exactly. If small damping is considered, they become nonzero due to the small-angle scattering of phonons.

Acknowledgments

The authors wish to thank A P Tankeyev for the discussion of the results and his useful comments. The study was performed under the RAS plan on topic 01.2.006.13395 with support under Presidium RAS program 24, the leading scientific school HIII 3257.2008.2.

Appendix A. The energy conservation law and the group velocity of phonons in cubic crystals

Let us compare the expressions used in [15–17] for the analysis of the energy conservation law with the function $F_{\lambda_1\lambda_2}(\theta_2, \varphi_2, \theta_1, \varphi_1)$, which we have introduced in accordance with (19). In a long-wavelength approximation ($q_1 \rightarrow 0$) the function $\Omega_{\lambda_1\lambda_2}$, which is given by

$$\begin{aligned} \Omega_{\lambda_1\lambda_2} &= \left(\omega_{q_1}^{\lambda_1} + \omega_{q_2}^{\lambda_2} - \omega_{q_1+q_2}^{\lambda_2} \right) \\ &= \omega_{q_1}^{\lambda_1} \left[1 - \frac{\omega_{q_1+q_2}^{\lambda_2} - \omega_{q_2}^{\lambda_2}}{\omega_{q_1}^{\lambda_1}} \right], \end{aligned} \quad (\text{A.1})$$

can be expressed in terms of the group velocity of phonons $V_{g_2}^{\lambda_2}$:

$$\Omega_{\lambda_1\lambda_2} = \omega_{q_1}^{\lambda_1} W_{\lambda_1\lambda_2}(\theta_1, \varphi_1, \theta_2, \varphi_2),$$

$$W_{\lambda_1\lambda_2}(\theta_1, \varphi_1, \theta_2, \varphi_2) = 1 - \frac{1}{S^{\lambda_1}(\theta_1, \varphi_1)} \left(\mathbf{V}_{g_2}^{\lambda_2}(\theta_2, \varphi_2) \cdot \mathbf{n}_1 \right). \quad (\text{A.2})$$

The group velocity of phonons can be written in the form

$$V_{g_2}^{\lambda_2}(\theta_2, \varphi_2) = S^{\lambda_2}(\theta_2, \varphi_2) \left\{ \mathbf{n}_2 + S_{\theta_2}^{\lambda_2} \mathbf{e}_{\theta_2} + S_{\varphi_2}^{\lambda_2} \mathbf{e}_{\varphi_2} \right\}, \quad (\text{A.3})$$

where

$$\begin{aligned} \mathbf{n}_2 &= \{ \sin \theta_2 \cos \varphi_2, \sin \theta_2 \sin \varphi_2, \cos \theta_2 \}, \\ \mathbf{e}_{\theta_2} &= \{ \cos \theta_2 \cos \varphi_2, \cos \theta_2 \sin \varphi_2, -\sin \theta_2 \}, \\ \mathbf{e}_{\varphi_2} &= \{ -\sin \varphi_2, \cos \varphi_2, 0 \}, \\ S_{\theta_2}^{\lambda_2} &= \frac{1}{S^{\lambda_2}} \frac{\partial S^{\lambda_2}}{\partial \theta_2} = \frac{\partial}{\partial \theta_2} \ln S^{\lambda_2}, \\ S_{\varphi_2}^{\lambda_2} &= \frac{1}{\sin \theta_2} \frac{1}{S^{\lambda_2}} \frac{\partial S^{\lambda_2}}{\partial \varphi_2}. \end{aligned} \quad (\text{A.4})$$

It is easy to verify that the vectors \mathbf{n}_2 , \mathbf{e}_{θ_2} and \mathbf{e}_{φ_2} form a mutually orthogonal system of unit vectors. In arbitrary directions of unit wavevectors of phonons \mathbf{n}_1 and \mathbf{n}_2 we have

$$\begin{aligned} W_{\lambda_1\lambda_2}(\theta_1, \varphi_1, \theta_2, \varphi_2) &= 1 - \frac{S^{\lambda_2}(\theta_2, \varphi_2)}{S^{\lambda_1}(\theta_1, \varphi_1)} \\ &\times \left\{ \cos \theta_{12} + S_{\theta_2}^{\lambda_2}(\theta_2, \varphi_2) [\sin \theta_1 \cos \theta_2 \cos(\varphi_2 - \varphi_1) \right. \\ &\left. - \sin \theta_2 \cos \theta_1] + S_{\varphi_2}^{\lambda_2}(\theta_2, \varphi_2) [\sin \theta_1 \sin(\varphi_1 - \varphi_2)] \right\}. \end{aligned} \quad (\text{A.5})$$

In the [001] direction ($\theta_1 = 0, \varphi_1 = 0$) it follows from (A.5) that

$$W_{\lambda\lambda_2}(0, 0, \theta_2, \varphi_2) = 1 - S^{\lambda_2}(\theta_2, \varphi_2) [\cos \theta_2 - S_{\theta_2}^{\lambda_2} \sin \theta_2] / S_{100}^{\lambda_2}. \quad (\text{A.6})$$

Expression (A.6) is used in [15–17] for calculating the energy conservation contours in all symmetric directions ([001], [101] and [111]). However, it holds for the [001] direction only. Its use for the other symmetric directions, as in [15–17], is erroneous. For example, in the [101] direction ($\theta_1 = \pi/4, \varphi_1 = 0$) it follows from (A.5) that

$$\begin{aligned} W_{\lambda_1\lambda_2}(\theta_1, \varphi_1, \theta_2, \varphi_2) &= 1 - \frac{S^{\lambda_2}(\theta_2, \varphi_2)}{\sqrt{2} S^{\lambda_1}(\theta_1, \varphi_1)} \\ &\times \left\{ \sin \theta_2 \cos \varphi_2 + \cos \theta_2 \right. \\ &\left. + S_{\theta_2}^{\lambda_2}(\theta_2, \varphi_2) (\cos \theta_2 \cos \varphi_2 - \sin \theta_2) - S_{\varphi_2}^{\lambda_2} \sin \varphi_2 \right\}. \end{aligned} \quad (\text{A.7})$$

Obviously, expressions (A.6) and (A.7) for the function $W_{\lambda_1\lambda_2}(\theta_1, \varphi_1, \theta_2, \varphi_2)$ are considerably different. Therefore, the analysis of the conservation law and the ultrasound absorptions [15–17] in the [101] and [111] directions is incorrect. Let us determine $S_{\theta}^{\lambda}(\theta, \varphi)$ and $S_{\varphi}^{\lambda}(\theta, \varphi)$ entering into expressions (A.2)–(A.7):

$$\begin{aligned} S_{\theta}^{\lambda}(\theta, \varphi) &= \frac{1}{S^{\lambda}} \frac{\partial S^{\lambda}}{\partial \theta} = \frac{1}{S^{\lambda}} \left(\frac{\partial S^{\lambda}}{\partial \xi} \frac{\partial \xi}{\partial \theta} + \frac{\partial S^{\lambda}}{\partial \eta} \frac{\partial \eta}{\partial \theta} \right), \\ S_{\varphi}^{\lambda}(\theta, \varphi) &= \frac{1}{\sin \theta \cdot S^{\lambda}} \left(\frac{\partial S^{\lambda}}{\partial \xi} \frac{\partial \xi}{\partial \varphi} + \frac{\partial S^{\lambda}}{\partial \eta} \frac{\partial \eta}{\partial \varphi} \right) \\ \frac{1}{S^{\lambda}} \frac{\partial S^{\lambda}}{\partial \xi} &= \left[\left(\frac{S_{100}^{\lambda}}{S^{\lambda}} \right)^2 \frac{c_{11} - c_{44}}{2c_{44}} Z_{\lambda} \right] \frac{1.5(k^2 - 1)}{r^2} \\ &\times \left\{ 1 - \frac{1.5(k^2 - 1)\xi + 13.5(k - 1)^2(1 + 2k)}{(1 - q^2)^{1/2}(r)^3} \right. \\ &\left. \times \operatorname{tg} \left(\frac{Q}{3} \mp \frac{2\pi}{3} \right) \right\} \\ \frac{1}{S^{\lambda}} \frac{\partial S^{\lambda}}{\partial \eta} &= \left[\left(\frac{S_{100}^{\lambda}}{S^{\lambda}} \right)^2 \frac{c_{11} - c_{44}}{2c_{44}} Z_{\lambda} \right] \\ &\times \frac{4.5(k^2 - 1)^2(1 + 2k)}{(1 - q^2)^{1/2}(r)^3} \operatorname{tg} \left(\frac{Q}{3} \mp \frac{2\pi}{3} \right), \end{aligned} \quad (\text{A.8})$$

$$\frac{\partial \xi}{\partial \theta} = \sin 2\theta [\cos 2\theta + 0.5(\sin \theta)^2(\sin 2\varphi)^2],$$

$$\frac{\partial \xi}{\partial \varphi} = 0.5(\sin \theta)^4 \sin 4\varphi,$$

$$\frac{\partial \eta}{\partial \theta} = \frac{1}{4} \sin 2\theta (\sin \theta)^2 [3(\cos \theta)^2 - 1] (\sin 2\varphi)^2,$$

$$\frac{\partial \eta}{\partial \varphi} = \frac{1}{2} (\sin \theta)^4 (\cos \theta)^2 \sin 4\varphi.$$

The expressions for Z_{λ} , q and r are given by formulae (5). The quantities $F_{\lambda_1\lambda_2}(\theta_1, \varphi_1, \theta_2, \varphi_2)$ and $\Delta_{\lambda_2}(\theta_1, \varphi_1, \theta_2, \varphi_2)$ introduced by us can be presented in terms of the above-defined quantities in the form

$$F_{\lambda_1\lambda_2}(\theta_1, \varphi_1, \theta_2, \varphi_2) = -\frac{S_1^{\lambda_1}}{S_2^{\lambda_2}} W_{\lambda_1\lambda_2}(\theta_1, \varphi_1, \theta_2, \varphi_2) \quad (\text{A.9})$$

$$\begin{aligned} \Delta_{\lambda_2}(\theta_1, \varphi_1, \theta_2, \varphi_2) &= S_{\theta_2}^{\lambda_2}(\mathbf{e}_{\theta_2} \mathbf{n}_1) + S_{\varphi_2}^{\lambda_2}(\mathbf{e}_{\varphi_2} \mathbf{n}_1) \\ &= S_{\theta_2}^{\lambda_2}(\theta_2, \varphi_2) [\sin \theta_1 \cos \theta_2 \cos(\varphi_2 - \varphi_1) + \\ &\quad - \sin \theta_2 \cos \theta_1] + S_{\varphi_2}^{\lambda_2}(\theta_2, \varphi_2) [\sin \theta_1 \sin(\varphi_2 - \varphi_1)]. \end{aligned} \quad (\text{A.10})$$

References

- [1] Kuleyev I G and Kuleyev I I 2007 *Fiz. Tverd. Tela, St. Petersburg* **49** 7 1272 (in Russian)
- [2] Kuleyev I G, Kuleyev I I and Arapova I Yu 2007 *J. Phys.: Condens. Matter* **19** 406216
- [3] Landau L and Rumer J 1937 *Sov. Phys.* **11** 18 (in Russian)
- [4] Truel B, Elbaum C and Chick B B 1969 *Ultrasonic Methods in Solid State Physics* (New York: Academic)
- [5] Tucker J W and Rampton V W 1972 *Microwave Ultrasonics in Solid State Physics* (Amsterdam: North-Holland)
- [6] Gurevich V L 1980 *Kinetics of Phonon Systems* (Moscow: Nauka) (in Russian)

- [7] Maris H J 1971 *Phys. Acoustics* **VIII** 279
- [8] Zhernov P and Inyushkin A V 2001 *Usp. Fiz. Nauk* **171** 827 (in Russian)
Zhernov P and Inyushkin A V 2002 *Usp. Fiz. Nauk* **172** 573 (in Russian)
- [9] Mogilyovsky B M and Chudnovsky A F 1972 *Thermal Conductivity of Semiconductors* (Moscow: Nauka) (in Russian)
- [10] Berman R 1976 *Thermal Conduction in Solids* (Oxford: Clarendon)
Berman R 1962 *Thermal Conduction in Solids* (Moscow: Mir) (in Russian)
- [11] Zhernov A P and Inyushkin A V 2001 *Isotope Effects in Solids* (Moscow: Ross. Nauchn. Tsentr Kurchatovski Institut) (in Russian)
- [12] Hamilton R A H and Parrot J E 1969 *Phys. Rev.* **178** 1284
- [13] Herring C 1954 *Phys. Rev.* **95** 4 954
- [14] Simons S 1957 *Proc. Camb. Phil. Soc.* **53** 6 702
- [15] King P J 1971 *J. Phys. C: Solid State Phys.* **4** 1306
- [16] Simpson I C 1975 *J. Phys. C: Solid State Phys.* **8** 399
- [17] Simpson I C 1975 *J. Phys. C: Solid State Phys.* **8** 1783
- [18] Fedorov F I 1965 *Theory of Elastic Waves in Crystals* (Moscow: Nauka) (in Russian)
Fedorov F I 1968 *Theory of Elastic Waves in Crystals* (New York: Plenum)
- [19] Kuleev I G and Kuleev I I 2007 *Fiz. Tverd. Tela, St. Petersburg* **49** 3 422 (in Russian)
- [20] Kittel C 1956 *Introduction to Solid State Physics* 2nd edn (New York: Wiley)
- [21] Mason W P 1965 *Phys. Acoustics* vol III, part B, p 235
- [22] Kuleev I G and Kuleev I I 2005 *Fiz. Tverd. Tela, St. Petersburg* **47** 2 300 (in Russian)
- [23] Ilisavski Yu V and Chiplis D 1972 *Fiz. Tverd. Tela, St. Petersburg* **14** 8 2412 (in Russian)
- [24] Ilisavski Yu V and Sternin V M 1985 *Fiz. Tverd. Tela, St. Petersburg* **27** 2 385 (in Russian)
- [25] Lemanov V V and Smolenskii G A 1972 *Usp. Fiz. Nauk* **108** 3 465 (in Russian)
- [26] Ahiezer A I 1938 *Zh. Exp. Teor. Phys.* **8** 1318 (in Russian)
Ahiezer A I 1939 *J. Phys. (USSR)* **1** 277
- [27] Frantsevich I N, Voronov F F and Bakuta S A 1982 *Elastic Constants and Modules of Elasticity of Metals and Nonmetals* (Kiev: Naukova dumka) (in Ukrainian)